Electronic Supplementary Material (ESI) for Organic & Biomolecular Chemistry.
This journal is © The Royal Society of Chemistry 2023

Supporting Information

S-Alkylation of dithiocarbamates via a hydrogen borrowing reaction strategy using alcohols as alkylating agents

Hima P,‡ Spandan Hati,‡ and Raju Dey*

Department of Chemistry, National Institute of Technology Calicut, Kozhikode, 673601, India

‡These two authors contributed equally to this work.

1	**General Information**	**2**
2	**State of Art**	**2**
3	**Experimental procedure**	**3-5**
4	**Controlled experiments**	**6**
5	**Materials characterization**	**7-12**
6	**Qualitative detection of hydrogen**	**13**
7	**Recyclability test of the catalyst**	**13**
8	**NMR data of compounds**	**14-21**
9	**^{1}H and ^{13}C NMR spectra**	**22-42**
10	**References**	**43-45**

1. General Information

All experiments were carried out under an inert argon atmosphere using an argon balloon (1atm). All the chromatographic solvents were distilled before use. Unless otherwise noted, all starting materials were purchased from commercial sources and used without any further purification. Analytical thin layer chromatography (TLC) was carried out on Merck 60 F254 pre-coated silica gel plate (0.2 mm thickness). All the products were isolated by chromatography on a silica gel (60-120 mesh) column using hexane and ethyl acetate as eluent.

^{1}H NMR spectra were recorded on JEOL 500 MHz NMR spectrometer. As an internal standard, chemical shifts of protons are calibrated using tetramethylsilane (TMS: δ 0.0 ppm). ^{13}C NMR spectra were recorded at a 125 MHz magnetic field and referenced to the carbon resonances of the solvent ($CDCl_3$: δ 77.0 ppm). Peaks are labeled as singlet (s), broad singlet (br), doublet (d), triplet (t), double doublet (dd), and multiplet (m). Deuterated chemicals were purchased from Cambridge Isotope Laboratories (CIL). High-resolution mass spectra (HRMS) were recorded on a MicroMass QTOF Mass Spectrometer ESI mode unless otherwise stated. The liberated gas is identified using GC chromatogram (Shimadzu GC-2010 Plus) by TCD detector.

2. State of art

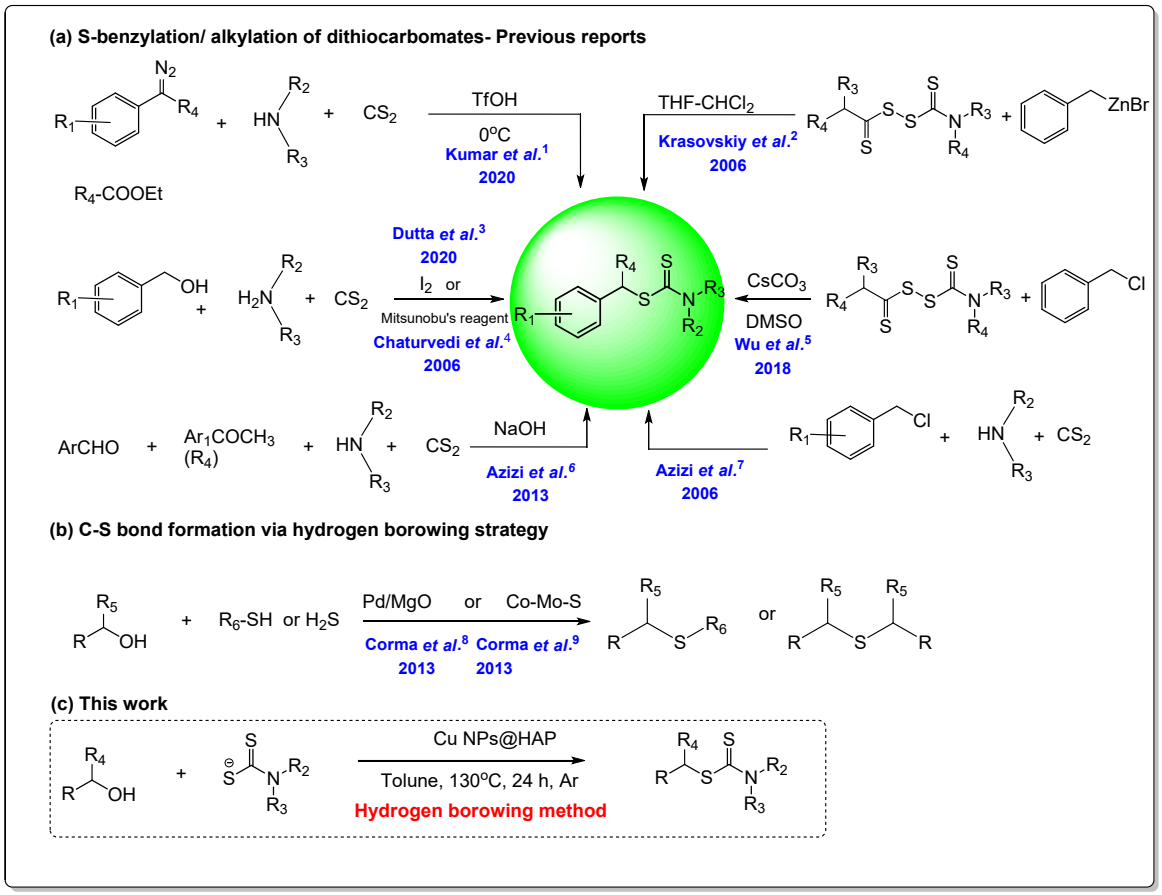

Scheme S1. a) Selected methods for S-benzylation/ alkylation of dithiocarbamate b) C-S bond formation via hydrogen borrowing strategy c) Present work

3. Experimental procedure

3.1. Synthesis of hydroxyapatite

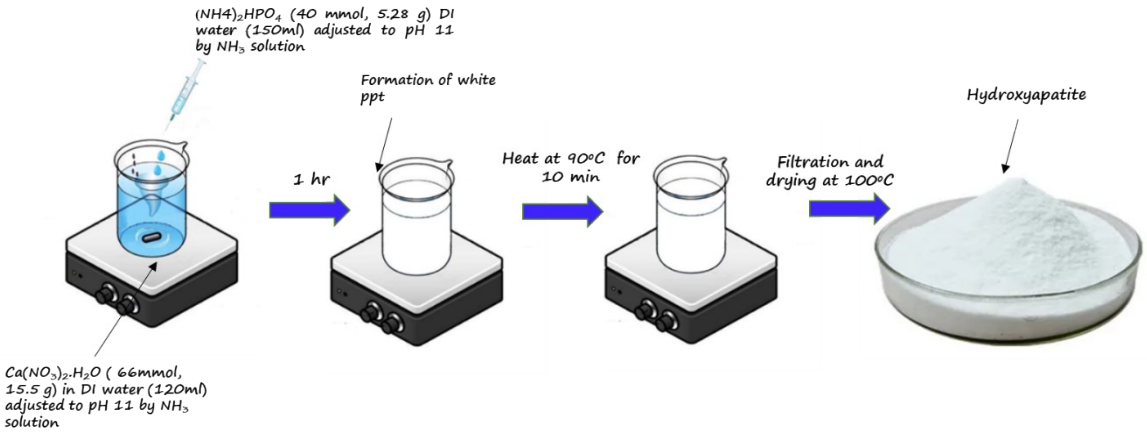

Scheme S2. Representative procedure for the synthesis of hydroxyapatite[14]

$(NH_4)_2HPO_4$ (40 mmol, 5.28 g) was dissolved in 150 mL of deionized water and the pH was adjusted to 11 with an aqueous ammonia solution. To an aqueous solution of $Ca(NO_3)_2.H_2O$ (66mmol, 15.5 g), aqueous ammonia solution was added dropwise to adjust the pH=11. Using a pressure equalizer $(NH_4)_2HPO_4$ solution was added dropwise to $Ca(NO_3)_2.H_2O$ solution at room temperature over a period of 30 minutes. The solution turned into milky white and was heated at 90°C for another 10 minutes. The precipitate formed was filtered, washed with deionized water, and dried, at 110°C.

3.2. Synthesis of hydroxyapatite-supported Cu nanoparticles.

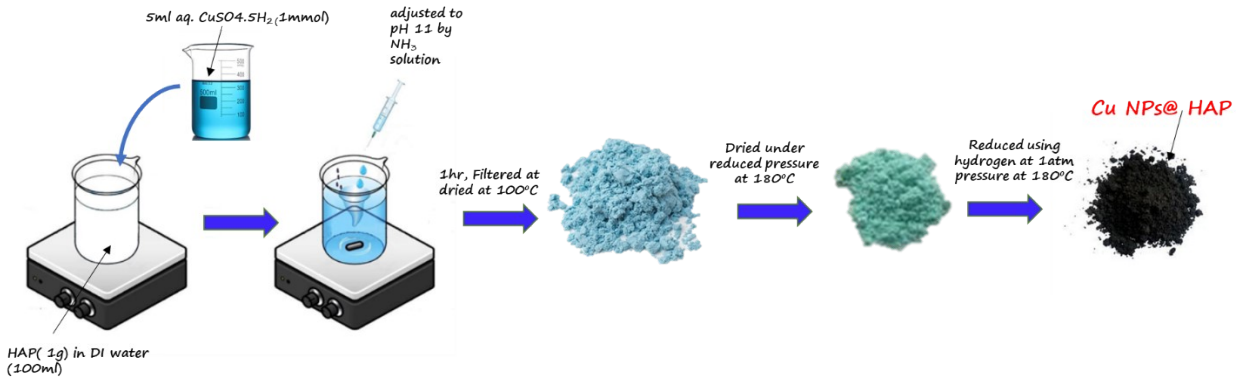

Scheme S3. Representative procedure for the synthesis of Cu NPs@HAP

$(NH_4)_2HPO_4$ (40 mmol, 5.28 g) was dissolved in 150 mL of deionized water and the pH was adjusted to 11 with an aqueous ammonia solution. To an aqueous solution of $Ca(NO_3)_2.H_2O$ (66mmol, 15.5 g), aqueous ammonia solution was added dropwise to adjust the pH=11. Using a pressure equalizer $(NH_4)_2HPO_4$ solution was added dropwise to $Ca(NO_3)_2.H_2O$ solution at room temperature over a period of 30 minutes. The solution turned into milky white and was heated at 90°C for another 10 minutes. The precipitate formed was filtered, washed with deionized water, and dried, at 110°C.

3.3. Experimental procedure for the S-alkylation of dithiocarbamate

Benzyl alcohol (0.5 mmol), dithiocarbamate salt (0.75 mmol), solvent (2ml), and catalyst (25mg) were taken in a reaction vessel. The reaction was stirred for the required time in a preheated heating block. After the reaction (TLC) was completed, the reaction vessel was

cooled to room temperature and diluted with 10 mL ethyl acetate. The reaction mixture was then filtered using celite. The filtrate was dried using a rotary evaporator, volatile impurities were removed under vacuum, and further purification of the product was carried out by silica gel column chromatography using hexane and ethyl acetate as eluent.

3.4. Gram scale synthesis of furan-2-ylmethyl diethylcarbamodithioate

Furfural alcohol (20 mmol), Sodium diethyldithiocarbamate (30 mmol), toluene (15 ml), and catalyst (150mg) were taken in a reaction vessel. The reaction was stirred for 24 hours in a preheated heating block (temperature of the metallic block at base: 130°C). After the reaction (TLC) was completed, the reaction vessel was cooled to room temperature and diluted with ethyl acetate. The reaction mixture was then filtered using celite. The filtrate was dried using a rotary evaporator, volatile impurities were removed under vacuum, and further purification of the product was carried out by silica gel column chromatography using hexane and ethyl acetate as eluent. The product furan-2-ylmethyl diethylcarbamodithioate was isolated with a yield of 65 % (2.97 g).

4. Controlled experiments

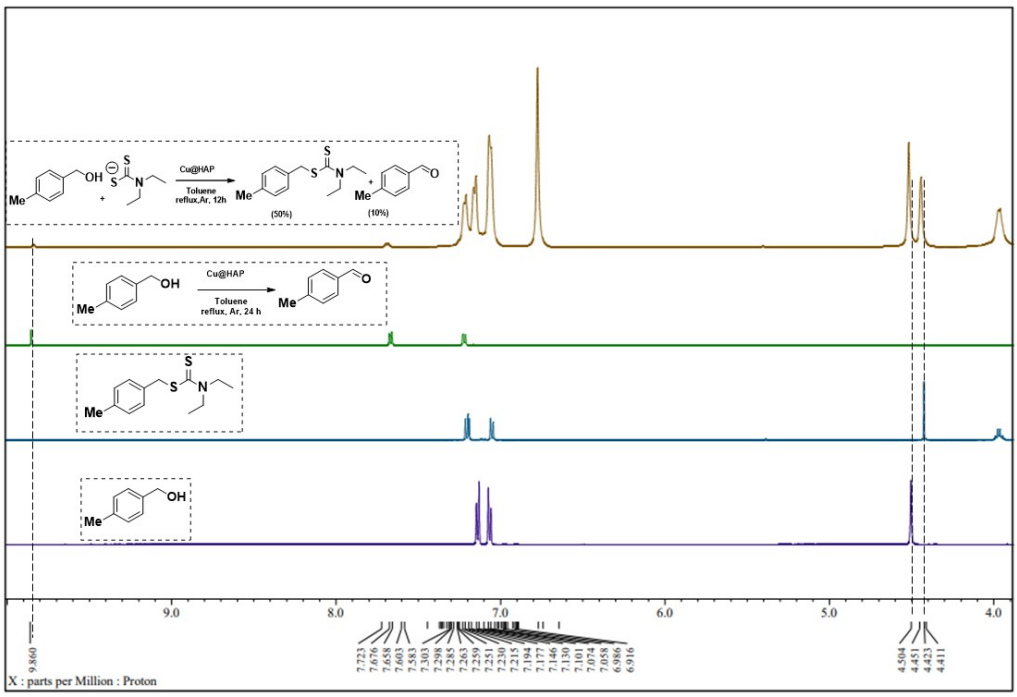

Figure S1. Controlled experiments and mechanistic investigation

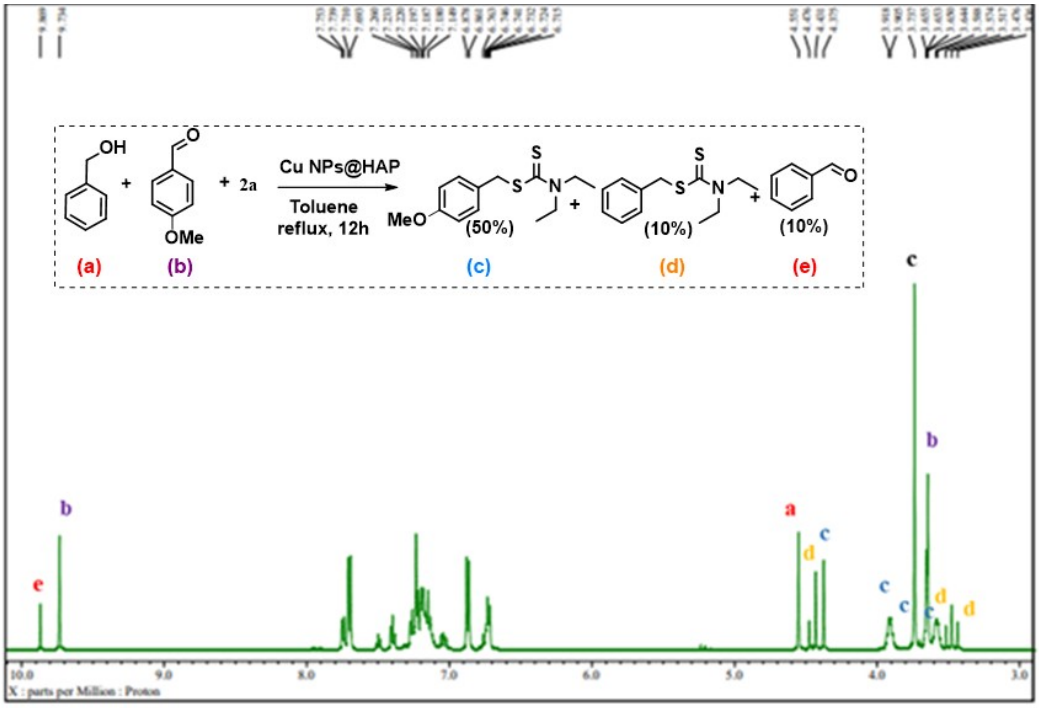

Figure S2. Crude NMR for the cross-over experiment between benzyl alcohol, 4-methoxy benzyl alcohol and sodium diethyldithiocarbamate

5. Materials characterization.

The synthesized copper loaded on hydroxyapatite was characterized using various analytical methods. The crystallinity and structural composition of the synthesized catalyst were ensured by X-ray diffraction (XRD) analysis at room temperature using a Malvern Pananalytical diffractometer with Cu Kα radiation source ($\lambda = 1.5406$ Å), operated at 45 kV and 40 mA. Fourier transform infrared equipped with FT-IR using KBr pellet was carried out using a Jasco FT/IR 4600 spectrometer. UV–vis by diffuse reflectance spectra were recorded between 200 and 3500 nm with a Perkin Elmer spectrometer UV/Vis (Lambda 750). The spectra were collected using $BaSO_4$ as the standard reference. Thermogravimetry/differential thermal analysis (TG/DTA) was performed using a Perkinelmer STA6000 apparatus. The experiments were conducted from room temperature until 700 °C under an air flow atmosphere at a constant heating rate of 10 °C.min^{-1}. Surface topology and morphology of particles were investigated using a Jeol JIB-4700F scanning electron microscope equipped with energy dispersive spectroscopy (SEM-EDS). The TEM micrographs were obtained on a JEOL JEM F200 high-resolution scanning/ transmission electron microscope. The copper content incorporated material was estimated by chemical analysis using inductively coupling plasma-atomic emission spectroscopy ICP-MS (Agilent 7800), after the acid digestion process. Surface chemical states were investigated by X-ray photoelectron spectroscopy (XPS) measurement with a Kratos analytical, AXIS Supra$^+$. The specific surface areas were determined from the nitrogen adsorption/desorption isotherms using the BET (Brunauer-Emmett-Teller) method.

5.1. Inductively coupled plasma (ICP) mass spectrometry analysis:

Inductively coupled plasma (ICP) mass spectrometry analysis was carried out to find the amount of copper present in the Cu NPs@HAP catalyst. The data showed a value of 5.7 wt% (0.89 $mmolg^{-1}$) for the copper present in the Cu NPs@ HAP catalyst.

5.2. UV-Visible spectra:

The UV-visible spectroscopic analysis was also carried out for Cu NPs@HAP catalysts, indicates the characteristic absorption peak at around 575 nm is possibly due to the surface plasmon band of Cu nanoparticle colloids supporting the formation of Cu NPs.[17]

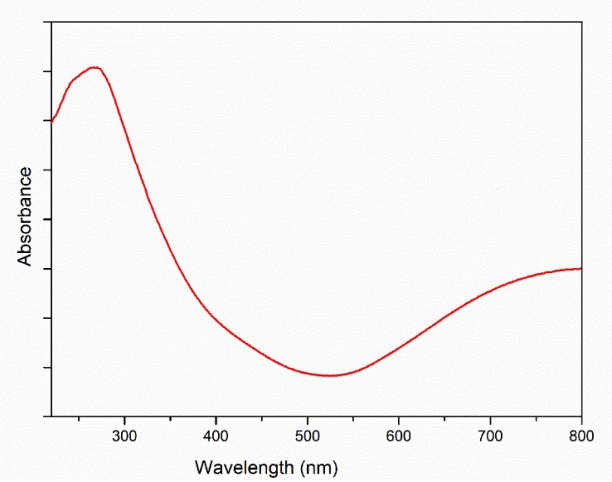

Figure S3. (a) The nature of the Cu species was determined by UV–vis spectroscopy. UV–vis by diffuse reflectance spectra were recorded between 200 and 3500 nm with a Perkin Elmer spectrometer UV/Vis (Lambda 750). The spectra were collected using $BaSO_4$ as the standard reference.

5.3. Thermal analysis:

The thermal stability of the Cu NPs@HAP was studied using thermogravimetric-differential scanning calorimetry at a heating rate of 10°C/min under an air atmosphere. The TGA-DSC plot of copper-incorporated hydroxyapatite shows no significant weight loss up to 180 °C. The

weight loss after 180 °C to 650 °C can be due to the elimination of water molecules from hydroxyapatite.[16]

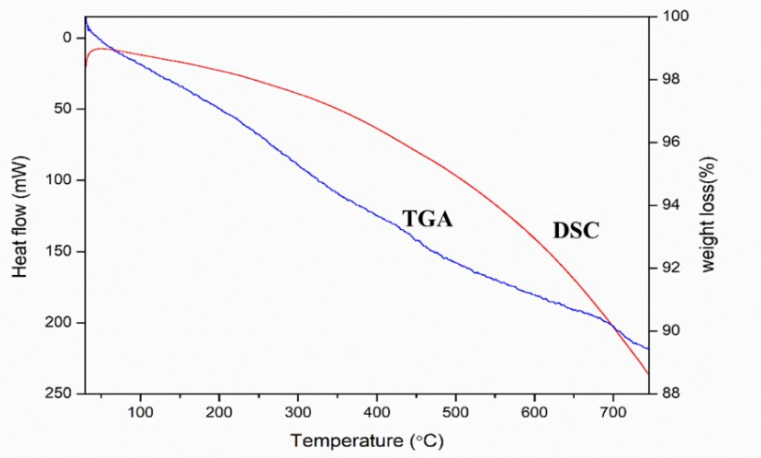

Figure S4. TGA and DSC curve for Cu NPs@ HAP using a Perkinelmer STA6000 apparatus. The experiments were conducted from room temperature until 700 °C under an air flow atmosphere at a constant heating rate of 10 °C.min^{-1}

5.4. N_2 adsorption-desorption isotherms:

Nitrogen adsorption–desorption isotherms of Cu NPs@HAP by Brunauer–Emmett–Teller method. The sharpness of the isotherms and the presence of type IV kind isotherms with hysteresis loop at $P/P_0 > 0.80$ suggest that the tested catalyst is mostly mesoporous.[15a]

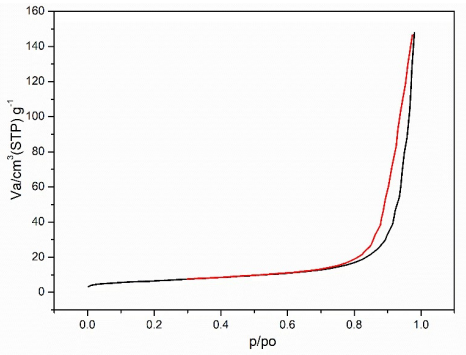

Figure. S5. N_2 adsorption-desorption isotherms for Cu NPs@ HAP catalyst determined using the BET (Brunauer-Emmett-Teller) method

Additionally, it has been found that Cu NPs/HAP catalyst has a BET-specific surface area of 23.265 [m^2g^{-1}] and means pore diameter of 39.337 nm which confirms the mesoporous structure of the material.[15b]

BET plot		
V_m	5.3453	[cm^3(STP) g^{-1}]
$a_{s,BET}$	23.265	[m^2 g^{-1}]
C	205.8	
Total pore volume(p/p_0=0.980)	0.2288	[cm^3 g^{-1}]
Mean pore diameter	39.337	[nm]

Table S1. Chemical analysis of copper, SBET area, pore diameter, and grain size of the catalyst by BET

5.5. Morphological analysis:

The morphology of the Cu NPs@HAP catalytic materials was analyzed by using scanning electron microscopy (SEM) and found it has a heterogeneous structure.

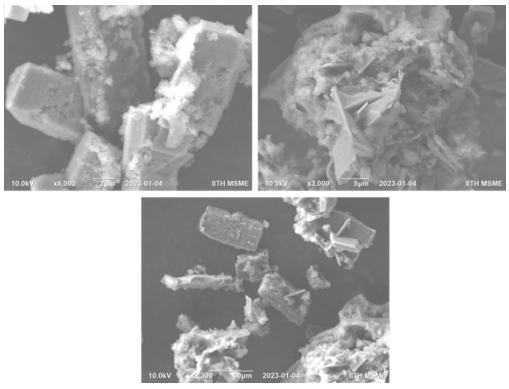

Figure S6. SEM image of copper on hydroxyapatite.

Furthermore, the elemental analysis by energy dispersive spectroscopy (EDS) of Cu NPs@HAP was also performed in different selected zones of the catalyst surface which confirmed the presence of elemental Ca, Cu, P, and O. From the analysis, the Ca/P was found to be in 1:1.7 ratio.

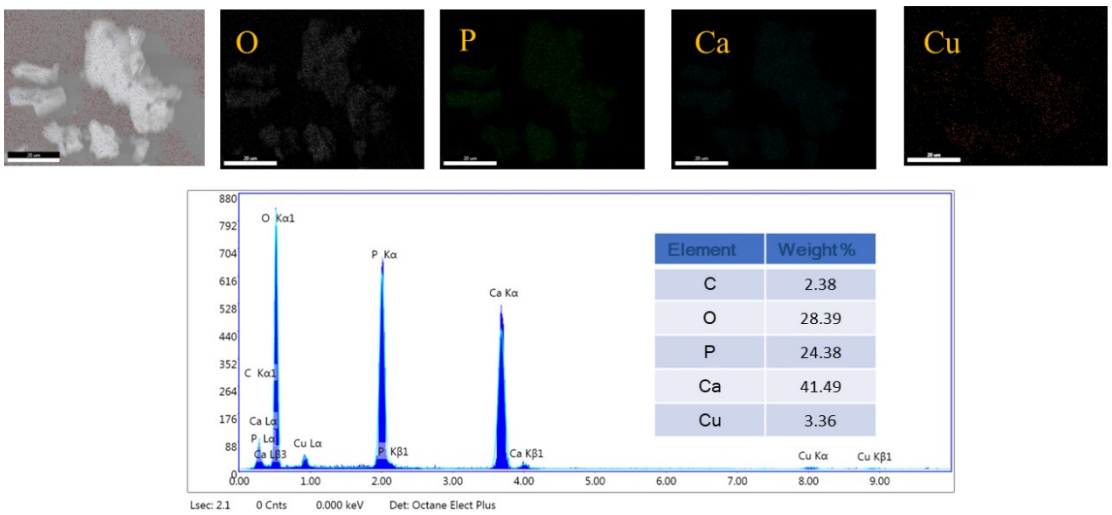

Figure S7. SEM- EDX mapping image of oxygen, phosphorus, calcium, and copper.

5.6. Structural studies:

The infrared (IR) technique is applied to confirm the surface's variation further.[18] The IR band observed at ~1038 cm^{-1} is due to the asymmetric stretching vibrations of P-O bond of PO_4^-. The peak at 3551 cm^{-1} corresponds to the OH group's stretching vibration present in the HAP structure. The peak at 1385 cm^{-1} appears due to the CO_3^{2-} species in hydroxyapatite. The broad peak appeared at 3100-3300 cm^{-1} and the peak at 1647 cm^{-1} represents the bending and stretching bands of H_2O molecules present in the material.[19] The disappearance of the H_2O peaks in the catalyst may be due to the loss of water molecules at high temperatures. Raman spectra of the catalyst is in full agreement with the IR data of the catalyst. The Raman spectrum of Cu NPs@HAP catalyst shows peaks at 1030, 1039, and 1066 cm^{-1} are identifying the asymmetric stretching mode(ν3) of the PO_4 group (O-P-O bond). The sharp intense peak at 957 cm^{-1} represents the symmetric stretching mode(ν1) of the PO_4 group (P–O bond). Due to the bending mode of the PO_4 group (O–P–O bond), the peaks at 588 and 602 cm^{-1}(ν4) and 424 cm^{-1} (ν2) appeared.[19]

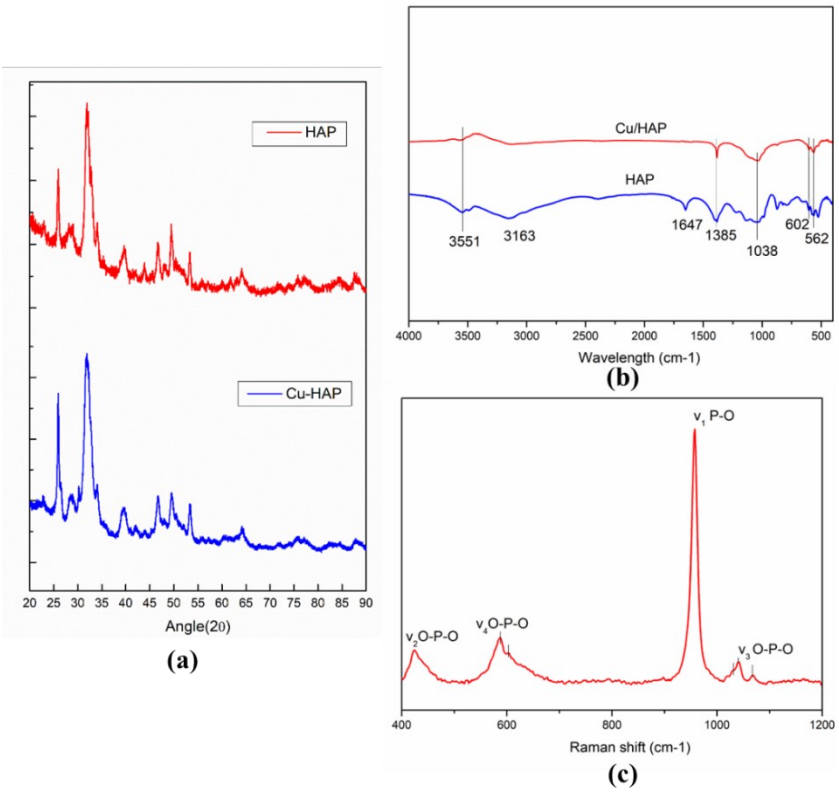

Figure S8. a) XRD spectra of the material analysed at room temperature using a Malvern P ananlytical diffractometer with Cu Kα radiation source ($\lambda = 1.5406$ Å), operated at 45 kV and 40 mA. b) Raman spectra of Cu NPs@HAP c) FTIR spectra of the HAP and Cu NPs@HAP spectra recorded at 25 °C.

5.7. Elemental analysis:

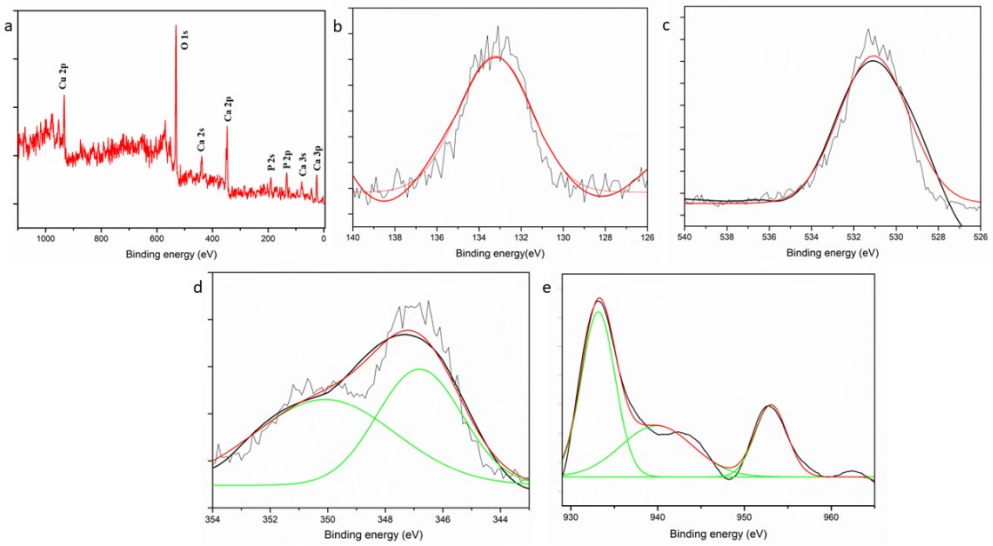

Figure S9. Surface chemical composition was measured through XPS (**a**) Full XPS spectra measured for Cu NPs@HAP b) P 2p, c) O 1s d) Ca 2p, d) Cu 2p

6. Qualitative detection of hydrogen

Benzyl alcohol (0.5 mmol), and Cu NPs@HAP (25mg) were added to an oven-dried reaction vessel containing a magnetic bar. To this, 2.0 mL of toluene was added. The reaction mixture was purged with argon and closed using a septum. The reaction was stirred in a preheated heating block. After 2 hrs, the gas collected using a syringe was subjected to GC analysis, and the retention time matched with a sample collected from a hydrogen cylinder of 99.9% purity.

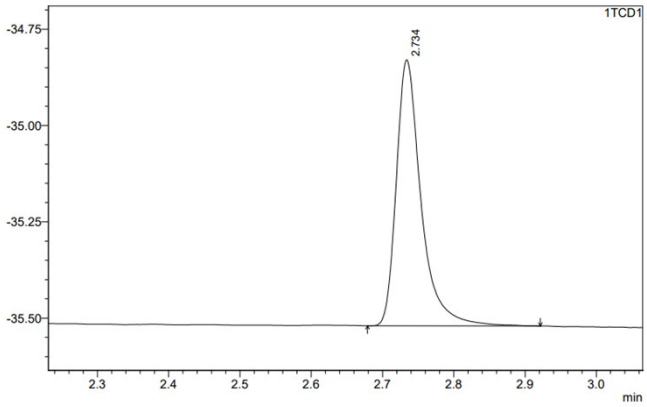

Figure S10. GC Spectrum for evolved gas (TCD mode).

7. Recyclability test of the catalyst.

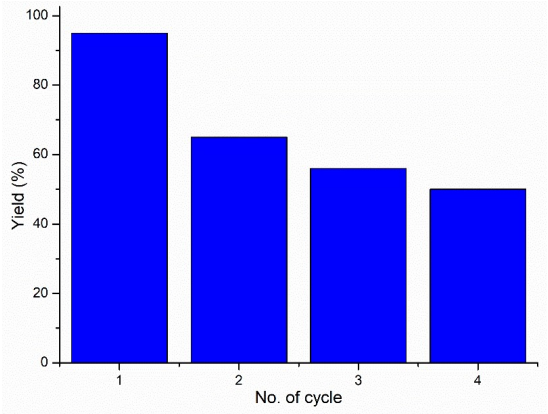

Figure S12. Recyclability test of the catalyst.

The catalyst has been tested for further cycles. It was found that the activity of the catalyst was slowly decreasing may be due to the agglomeration of the nanoparticle.

8. NMR data of compounds in Table 2

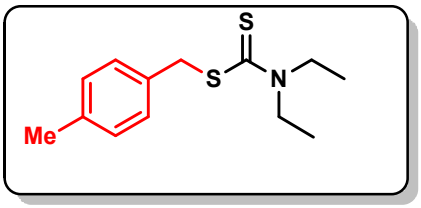	**4-methylbenzyl diethylcarbamodithioate (3a, table 2)[9]** Eluent: Hexane/ Ethyl acetate (98:1), Yellow oil (85%) ^{1}H NMR (500 MHz, $CDCl_3$) δ 7.21-7.19 (m, 2H), 7.05 (d, *J* = 7.8 Hz, 2H), 4.42 (s, 2H), 3.97 (q, *J* = 7.0 Hz, 2H), 3.64 (q, *J* = 7.1 Hz, 2H), 2.26 (s, 3H), 1.20 (dd, J = 15.6, 7.2 Hz, 6H) ^{13}C NMR (125 MHz, $CDCl_3$) δ 195.4, 137.2, 132, 129.3, 129.2, 49.3, 46.6, 42.0, 21.1, 12.4, 11.5
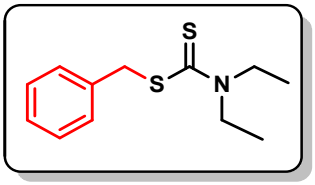	**benzyl diethylcarbamodithioate (3b, Table 2)[9]** Eluent: Hexane/ Ethyl acetate (98:2)), colourless oil (82%) ^{1}H NMR (500 MHz, $CDCl_3$) δ 7.31 (d, *J* = 7.2 Hz, 2H), 7.24-7.22 (m, 2H), 7.19-7.16 (m, 1H), 4.47 (s, 2H), 3.97 (d, *J* = 6.9 Hz, 2H), 3.65 (d, *J* = 6.7 Hz, 2H), 1.20 (q, *J* = 6.7 Hz, 6H) ^{13}C NMR (125 MHz, $CDCl_3$) δ 195.2, 135.9, 129.3, 128.5, 127.4, 49.4, 46.6, 42.1, 12.4, 11.5
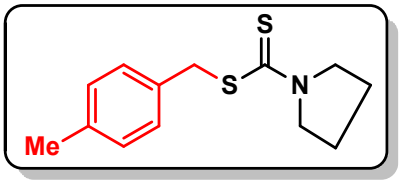	**4-methylbenzyl pyrrolidine-1-carbodithioate (3c, table 2)[9]** Eluent: Hexane/ Ethyl acetate (98:1), Yellow oil (85%) ^{1}H NMR (500 MHz, $CDCl_3$) δ 7.24 (d, *J* = 7.8 Hz, 2H), 7.16 (d, *J* = 8.0 Hz, 2H), 4.62 (s, 2H), 3.60-3.58 (m, 4H), 2.34 (s, 3H), 1.90-1.87 (m, 4H) ^{13}C NMR (125 MHz, $CDCl_3$) δ 184.5, 137.9, 137.3, 129.1, 127.0, 65.0, 52.8, 25.6, 21.1

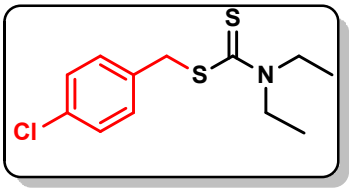	**4-chlorobenzyl diethylcarbamodithioate (3d, table 2)[9]** Eluent: Hexane/ Ethyl acetate (98:2), Colourless liquid (85%) ^{1}H NMR (500 MHz, $CDCl_3$) δ 7.27-7.22 (m, 2H), 7.22-7.19 (m, 2H), 4.45 (s, 2H), 3.97 (q, *J* = 7.1 Hz, 2H), 3.65 (q, *J* = 7.1 Hz, 2H), 1.23-1.19 (m, 6H) ^{13}C NMR (125 MHz, $CDCl_3$) δ 194.7, 134.9, 133.2, 130.7, 128.7, 49.6, 46.7, 41.2, 12.5, 11.6
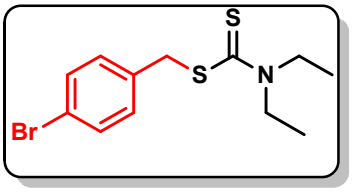	**4-bromobenzyl diethylcarbamodithioate (3e, table 2)[9]** Eluent: Hexane/ Ethyl acetate (98:2), Colourless liquid (79%) ^{1}H NMR (500 MHz, $CDCl_3$) δ 7.26-7.24 (m, 2H), 7.20 (t, *J* = 2.1 Hz, 1H), 7.19 (d, *J* = 1.3 Hz, 1H), 4.45 (s, 2H), 3.96 (d, *J* = 7.1 Hz, 2H), 3.65 (d, *J* = 7.1 Hz, 2H), 1.20 (t, *J* = 7.1 Hz, 6H) ^{13}C NMR (125 MHz, $CDCl_3$) δ 194.7, 135.0, 133.2, 130.6, 128.6, 49.6, 46.7, 41.1, 12.5, 11.5
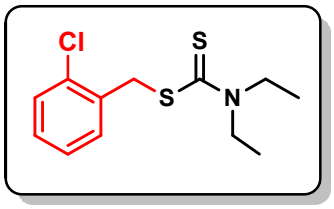	**2-chlorobenzyl diethylcarbamodithioate (3f, table 2)[9]** Eluent: Hexane/ Ethyl acetate (25:1), Yellow oil (75%) ^{1}H NMR (500 MHz, $CDCl_3$) δ 7.49 (dd, *J* = 5.7, 3.6 Hz, 1H), 7.29 (dd, *J* = 5.6, 3.7 Hz, 1H), 7.13 (dd, *J* = 5.8, 3.5 Hz, 2H), 4.62 (s, 2H), 3.97 (d, *J* = 7.1 Hz, 2H), 3.65 (d, *J* = 7.2 Hz, 2H), 1.20 (t, *J* = 7.2 Hz, 6H) ^{13}C NMR (125 MHz, $CDCl_3$) δ 195.0, 134.5, 134.4, 131.5, 129.5, 128.9, 126.9, 49.6, 46.7, 39.6, 12.5, 11.6

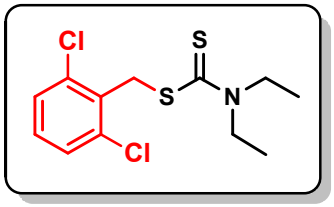	**2,6-dichlorobenzyl diethylcarbamodithioate (3g, table 2)[20]** Eluent: Hexane/ Ethyl acetate (25:1), colourless oil (86%) ^{1}H NMR (500 MHz, $CDCl_3$) δ 7.25 (d, *J* = 8.0 Hz, 2H), 7.10 (dd, *J* = 8.4, 7.8 Hz, 1H), 4.68 (s, 2H), 3.98 (q, *J* = 6.9 Hz, 2H), 3.64 (q, *J* = 7.0 Hz, 2H), 1.25-1.18 (m, 6H) ^{13}C-NMR (125 MHz, $CDCl_3$) δ 194.7, 136.5, 131.5, 129.3, 128.3, 49.3, 46.8, 38.7, 12.4, 11.6
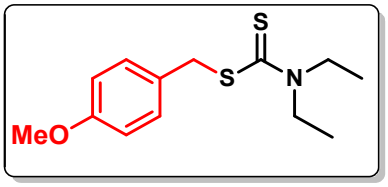	**4-methoxybenzyl diethylcarbamodithioate (3h, table 2)[13]** Eluent: Hexane/ Ethyl acetate (25:1), Colorless oil (86 %) ^{1}H-NMR (500 MHz, $CDCl_3$) δ 7.24 (dd, *J* = 6.7, 1.9 Hz, 2H), 6.78 (dd, J = 6.6, 2.0 Hz, 2H), 4.41 (s, 2H), 3.97 (d, *J* = 7.1 Hz, 2H), 3.72 (d, *J* = 3.2 Hz, 3H), 3.65 (d, *J* = 7.1 Hz, 2H), 1.23-1.18 (m, 6H) ^{13}C-NMR (125 MHz, $CDCl_3$) δ 195.4, 159.0, 130.5, 127.7, 114.0, 55.2, 49.3, 46.7, 41.8, 12.4, 11.6
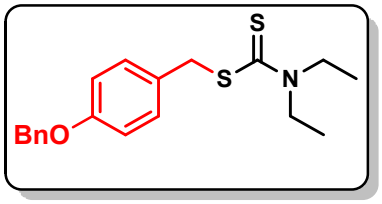	**4-(benzyloxy) benzyl diethylcarbamodithioate (3i, table 2)[11]** Eluent: Hexane/ Ethyl acetate (25:1), Colorless oil (79%) ^{1}H NMR (500 MHz, $CDCl_3$) δ 7.36-7.29 (m, 4H), 7.26-7.22 (m, 3H), 6.86-6.83 (m, 2H), 4.97 (s, 2H), 4.41 (s, 2H), 3.96 (q, *J* = 7.2 Hz, 2H), 3.64 (q, *J* = 7.1 Hz, 2H), 1.20 (dd, *J* = 15.7, 7.2 Hz, 6H) ^{13}C NMR (125 MHz, $CDCl_3$) δ 195.4, 158.2, 136.9, 130.6, 128.6, 128.0, 127.9, 127.4, 114.9, 70.0, 49.3, 46.7, 41.8, 12.4, 11.6

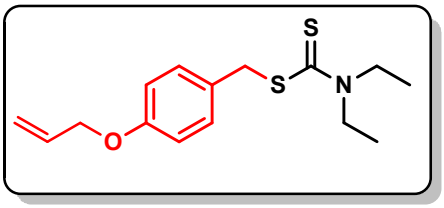	**4-(allyloxy) benzyl diethylcarbamodithioate (3j, table 2)** Eluent: Hexane/ Ethyl acetate (25:1) colourless oil (85 %) ^{1}H NMR (500 MHz, $CDCl_3$) δ 7.23-7.19 (m, 2H), 6.80-6.78 (m, 2H), 6.01-5.93 (m, 1H), 5.33 (dq, *J* = 17.2, 1.6 Hz, 1H), 5.21 (dq, *J* = 10.5, 1.3 Hz, 1H), 4.45 (dt, *J* = 5.3, 1.5 Hz, 2H), 4.41 (s, 2H), 3.97 (q, *J* = 7.0 Hz, 2H), 3.64 (q, *J* = 7.1 Hz, 2H), 1.20 (q, *J* = 7.4 Hz, 6H) ^{13}C NMR (125 MHz, $CDCl_3$) δ 195.4, 158.0, 133.2, 130.5, 127.9, 117.6, 114.8, 68.8, 49.3, 46.6, 41.8, 12.4, 11.6 HRMS (ESI) m/z: $[M+Na]^+$ calcd. for $C_{15}H_{21}NOS_2Na$ 318.0962; found 318.0962
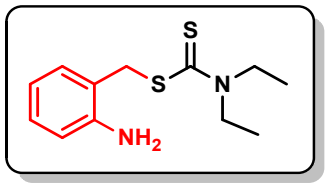	**2-aminobenzyl diethylcarbamodithioate (3k, table 2)** Eluent: Hexane/ Ethyl acetate (10:1), Yellow oil (79%) ^{1}H NMR (500 MHz, $CDCl_3$) δ 7.09-7.01 (m, 2H), 6.64-6.59 (m, 2H), 4.51 (s, 2H), 3.97 (q, *J* = 7.1 Hz, 2H), 3.66 (q, *J* = 7.0 Hz, 2H), 1.23-1.18 (m, 6H) ^{13}C NMR (125 MHz, $CDCl_3$) δ 195.4, 145.3, 131.1, 129.0, 119.2, 118.2, 115.7, 49.6, 46.7, 40.0, 12.4, 11.5 HRMS (ESI) m/z: $[M+H]^+$ calcd. for $C_{12}H_{18}N_2S_2H$ 255.0990; found 255.0993
	naphthalen-2-ylmethyl diethylcarbamodithioate (3l, table 2)[11] Eluent: Hexane/ Ethyl acetate (10:1), Yellow oil (79%) ^{1}H NMR (500 MHz, $CDCl_3$) δ 7.77 (s, 1H), 7.74-7.71 (m, 3H), 7.43-7.37 (m, 3H), 4.64 (s, 2H), 3.98

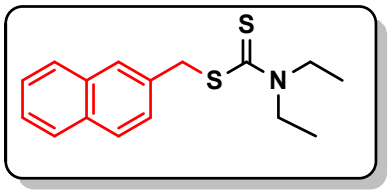	(d, *J* = 7.1 Hz, 2H), 3.65 (d, *J* = 7.2 Hz, 2H), 1.23-1.18 (m, 6H) ^{13}C NMR (126 MHz, $CDCl_3$) δ 195.1, 133.5, 133.3, 132.7, 128.3, 128.1, 127.6, 127.3, 127.2, 126.1, 125.9, 49.5, 46.7, 42.4, 12.5, 11.5
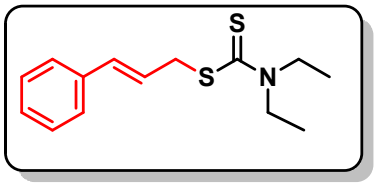	**cinnamyl diethylcarbamodithioate (3m, table 2)[10]** Eluent: Hexane/ Ethyl acetate (25:1), Yellow oil (82%) ^{1}H NMR (500 MHz, $CDCl_3$) δ 7.31-7.29 (m, 2H), 7.24-7.21 (m, 2H), 7.17-7.15 (m, 1H), 6.56 (d, *J* = 15.6 Hz, 1H), 6.28-6.23 (m, 1H), 4.10 (dd, *J* = 7.4, 1.1 Hz, 2H), 3.98 (d, *J* = 7.1 Hz, 2H), 3.68 (d, *J* = 7.1 Hz, 2H), 1.22 (dd, *J* = 11.1, 7.1 Hz, 6H) ^{13}C NMR (125 MHz, $CDCl_3$) δ 195.0, 136.7, 133.5, 128.5, 127.6, 126.4, 124.1, 49.5, 46.7, 40.2, 12.5, 11.6
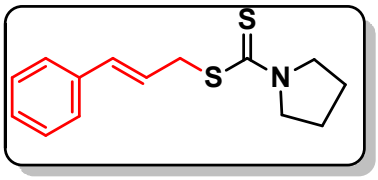	**cinnamyl pyrrolidine-1-carbodithioate (3n, table 2) [2]** Eluent: Hexane/ Ethyl acetate (25:1), Colourless liquid (80%) ^{1}H NMR (500 MHz, $CDCl_3$) δ 7.38-7.35 (m, 2H), 7.31-7.28 (m, 2H), 7.24-7.22 (m, 1H), 6.63 (d, *J* = 15.6 Hz, 1H), 6.35-6.31 (m, 1H), 4.19 (dd, *J* = 7.4, 1.1 Hz, 2H), 3.95 (t, *J* = 7.1 Hz, 2H), 3.66 (t, *J* = 6.9 Hz, 2H), 2.09-2.06 (m, 2H), 2.00-1.97 (m, 2H) ^{13}C NMR (125 MHz, $CDCl_3$) δ 192.2, 136.7, 133.4, 128.5, 127.6, 126.4, 124.2, 55.0, 50.6, 39.4, 26.1, 24.3
	1-phenylethyl diethylcarbamodithioate (3o, table 2)[11] Eluent: Hexane/ Ethyl acetate (25:1), Colourless oil

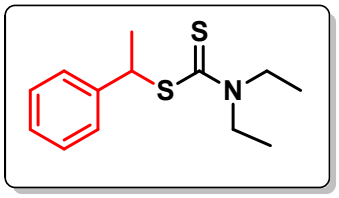	(82%) ^{1}H NMR (500 MHz, $CDCl_3$) δ 7.37-7.35 (m, 2H), 7.27-7.24 (m, 2H), 7.18 (dd, *J* = 5.5, 1.7 Hz, 1H), 5.20 (d, *J* = 7.1 Hz, 1H), 3.95 (d, *J* = 7.1 Hz, 2H), 3.62 (d, *J* = 7.1 Hz, 2H), 1.71 (d, *J* = 7.1 Hz, 3H), 1.21-1.16 (m, 6H) ^{13}C NMR (125 MHz, $CDCl_3$) δ 194.7, 142.2, 128.5, 127.9, 127.3, 50.8, 49.2, 46.6, 22.1, 12.5, 11.6
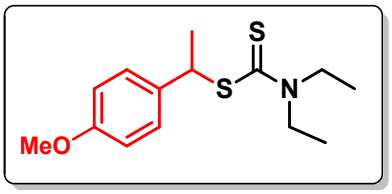	**1-(4-methoxyphenyl) ethyl diethylcarbamodithioate (3p, table 2)[13]** ^{1}H-NMR (500 MHz, $CDCl_3$) δ 7.29 (dd, *J* = 6.8, 2.0 Hz, 2H), 6.80-6.77 (m, 2H), 5.15 (d, *J* = 7.1 Hz, 1H), 3.95 (q, J = 7.0 Hz, 2H), 3.73 (s, 3H), 3.62 (q, J = 6.9 Hz, 2H), 1.70 (d, *J* = 7.1 Hz, 3H), 1.22-1.18 (m, 6H) ^{13}C-NMR (125MHz, $CDCl_3$) δ 194.8, 158.8, 134.1, 128.9, 113.8, 55.2, 50.3, 49.1, 46.6, 22.1, 12.5, 11.6
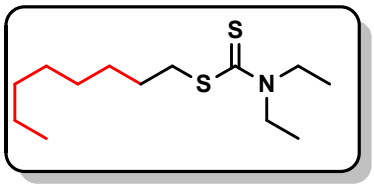	**Octyl diethylcarbamodithioate diethylcarbamodithioate (3q, table 2)[12]** Eluent: Hexane/ Ethyl acetate (25:1), Yellow oil (78 %) ^{1}H-NMR (500 MHz, $CDCl_3$) δ 3.97 (d, *J* = 7.1 Hz, 2H), 3.68 (d, *J* = 7.1 Hz, 2H), 3.20 (t, *J* = 7.4 Hz, 2H), 1.63 (q, *J* = 7.6 Hz, 2H), 1.34 (q, *J* = 7.4 Hz, 2H), 1.26-1.19 (m, 14H), 0.81 (t, *J* = 7.0 Hz, 3H) ^{13}C NMR (125 MHz, $CDCl_3$) δ 196.1, 49.3, 46.6, 37.3, 31.8, 29.7, 29.2, 29.1, 28.6, 22.6, 14.1, 12.4, 11.6
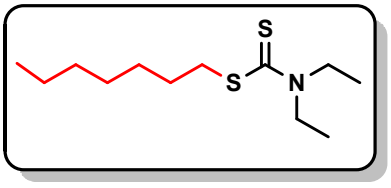	**heptyl diethylcarbamodithioate (3r, table 2)[12]** Eluent: Hexane/ Ethyl acetate (25:1), Yellow oil (80 %) ^{1}H-NMR (500 MHz, $CDCl_3$) δ 3.97 (q, *J* = 6.9 Hz,

	2H), 3.68 (q, J = 7.1 Hz, 2H), 3.20 (t, J = 7.4 Hz, 2H), 1.66-1.60 (m, 2H), 1.38-1.31 (m, 2H), 1.25-1.19 (m, 12H), 0.81 (t, J = 7.0 Hz, 3H) ^{13}C-NMR (125 MHz, $CDCl_3$) δ 195.1, 48.3, 45.6, 36.3, 30.7, 28.0, 27.9, 27.6, 21.6, 13.1, 11.4, 10.6.
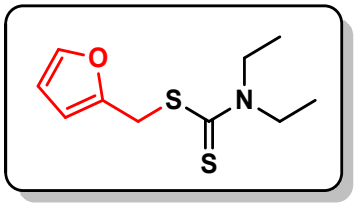	**furan-2-ylmethyl diethylcarbamodithioate (3s, table 2)** Eluent: Hexane/ Ethyl acetate (25:1), Yellow oil (82%) ^{1}H NMR (500 MHz, $CDCl_3$) δ 7.28 (q, J = 0.8 Hz, 1H), 6.25-6.23 (m, 2H), 4.55 (s, 2H), 3.95 (q, J = 7.0 Hz, 2H), 3.67-3.61 (m, 2H), 1.20 (t, J = 7.2 Hz, 6H) ^{13}C NMR (125 MHz, $CDCl_3$) δ 194.3, 149.6, 142.2, 110.5, 108.5, 49.5, 46.6, 34.4, 12.4, 11.5 HRMS (ESI) m/z: $[M+H]^+$ calcd. for $C_{10}H_{15}NOS_2H$ 230.0673; found 230.0676
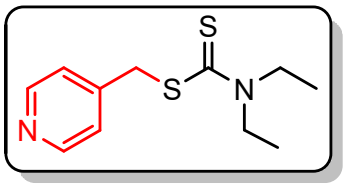	**pyridin-4-ylmethyl diethylcarbamodithioate (3t, table 2)** [21] Eluent: Hexane/ Ethyl acetate (25:1), White oil (70 %) ^{1}H NMR (500 MHz, $CDCl_3$) δ 8.51 (d, J = 5.3 Hz, 2H), 7.31 (d, J = 6.1 Hz, 2H), 4.56 (s, 2H), 4.03 (q, J = 7.1 Hz, 2H), 3.74 (q, J = 7.1 Hz, 2H), 1.30-1.24 (m, 6H) ^{13}C NMR (125 MHz, $CDCl_3$) δ 194.1, 149.8, 135.3, 124.3, 50.1, 46.9, 40.3, 12.7, 11.6
	Ferrocenyl diethylcarbamodithioate (3u, table 2) Eluent: Hexane/ Ethyl acetate (25:1), Yellow solid (80 %)

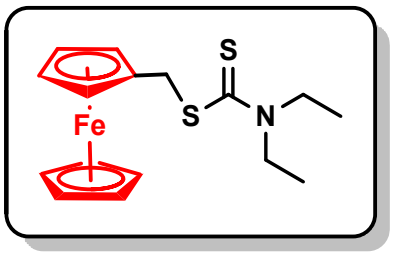	^{1}H NMR (500 MHz, $CDCl_3$) δ 4.26 (s, 2H), 4.20 (s, 2H), 4.12-4.10 (m, 5H), 4.06 (d, *J* = 1.7 Hz, 2H), 3.96 (t, *J* = 6.9 Hz, 2H), 3.64 (d, *J* = 7.1 Hz, 2H), 1.22-1.19 (m, 6H) ^{13}C NMR (125 MHz, $CDCl_3$) δ 195.5, 82.4, 69.1, 68.9, 68.1, 49.3, 46.6, 38.3, 12.4, 11.6 HRMS (ESI) m/z: $[M]^+$ calcd. for $C_{16}H_{21}FeNS_2$ 347.0465; Found 347.0471

9. ^{1}H and ^{13}C NMR spectra

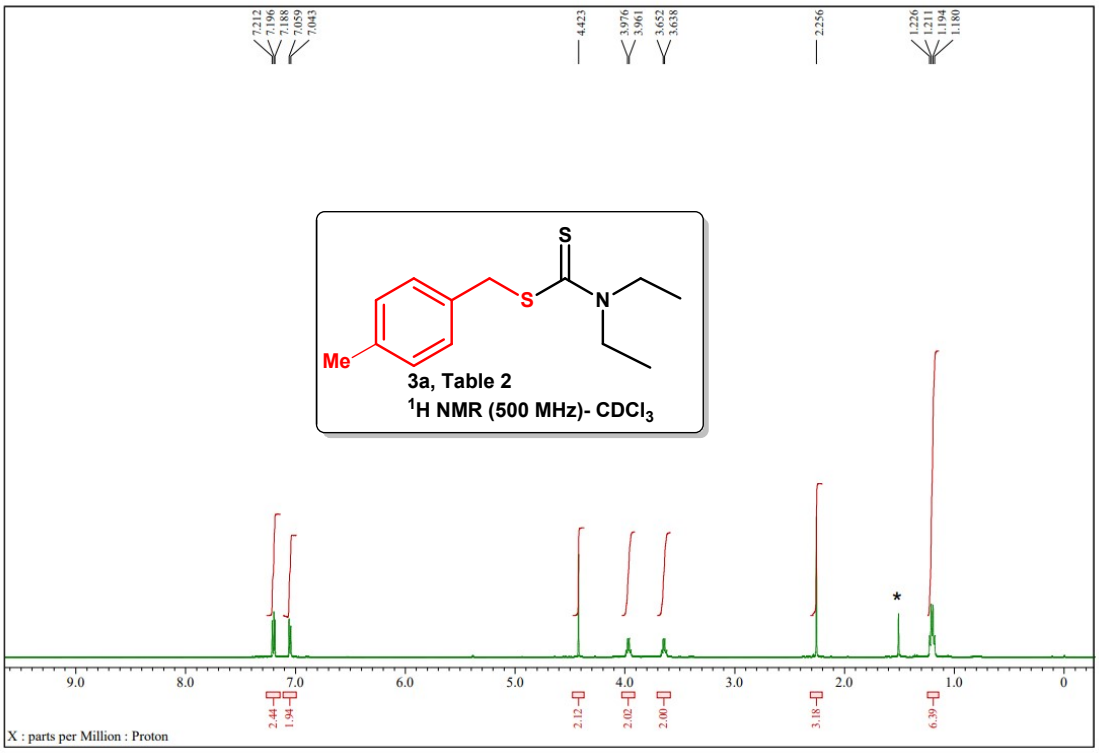
7.212
7.196
7.188
7.059
7.043
4.423
3.976
3.961
3.652
3.638
2.256
1.226
1.211
1.194
1.180
S
S
N
Me
3a, Table 2
1H NMR (500 MHz)- CDCl3
*
9.0
8.0
7.0
6.0
5.0
4.0
3.0
2.0
1.0
0
2.44
1.94
2.12
2.02
2.00
3.18
6.39
X : parts per Million : Proton

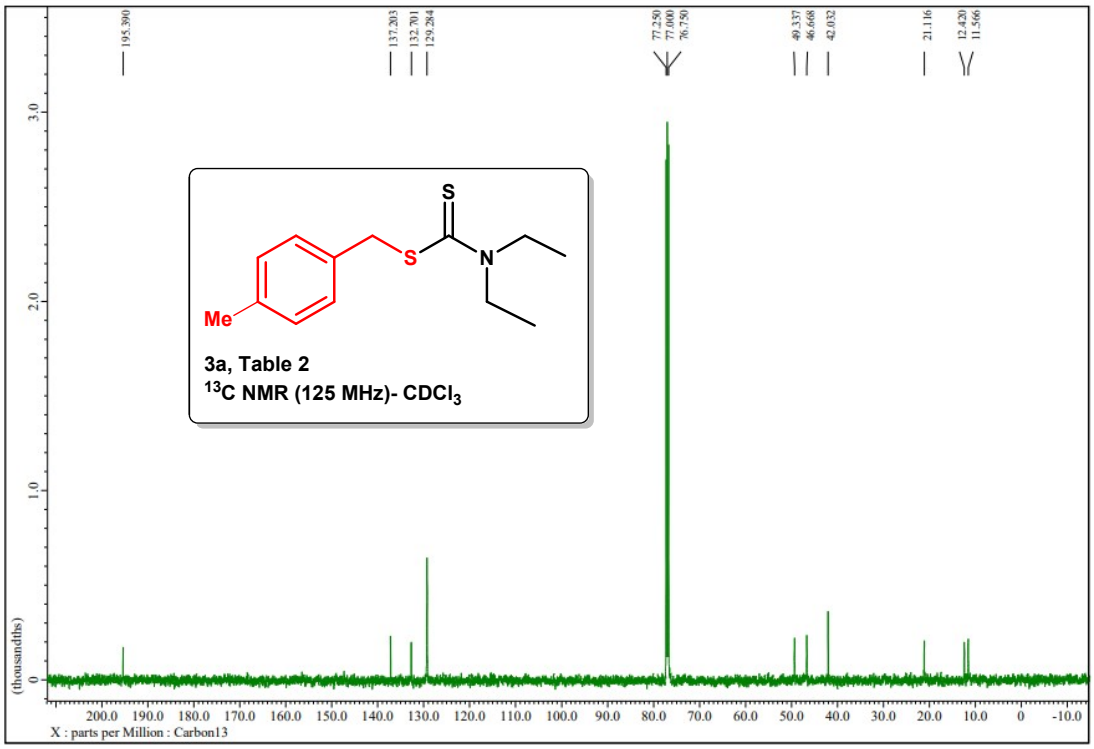
195.390
137.203
132.701
129.284
77.250
77.000
76.750
49.337
46.668
42.032
21.116
12.420
11.566
S
S
N
Me
3a, Table 2
13C NMR (125 MHz)- CDCl3
3.0
2.0
1.0
0
(thousandths)
200.0
190.0
180.0
170.0
160.0
150.0
140.0
130.0
120.0
110.0
100.0
90.0
80.0
70.0
60.0
50.0
40.0
30.0
20.0
10.0
0
-10.0
X : parts per Million : Carbon13

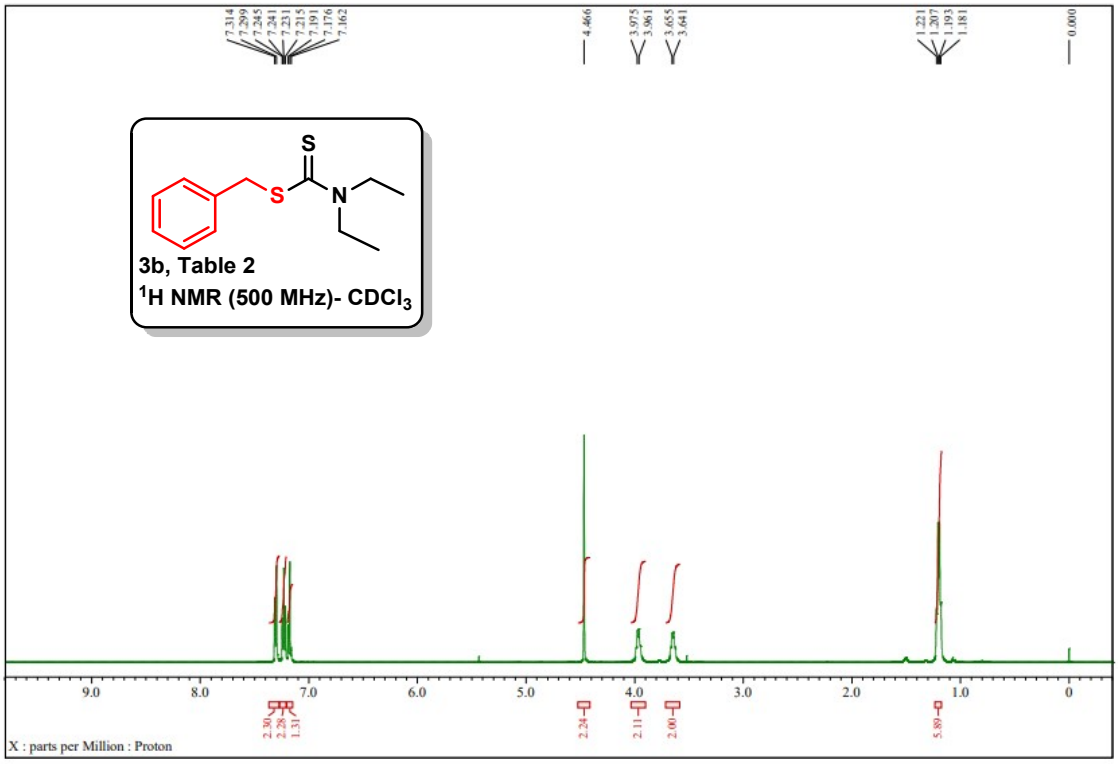
3b, Table 2
1H NMR (500 MHz)- CDCl3
X : parts per Million : Proton

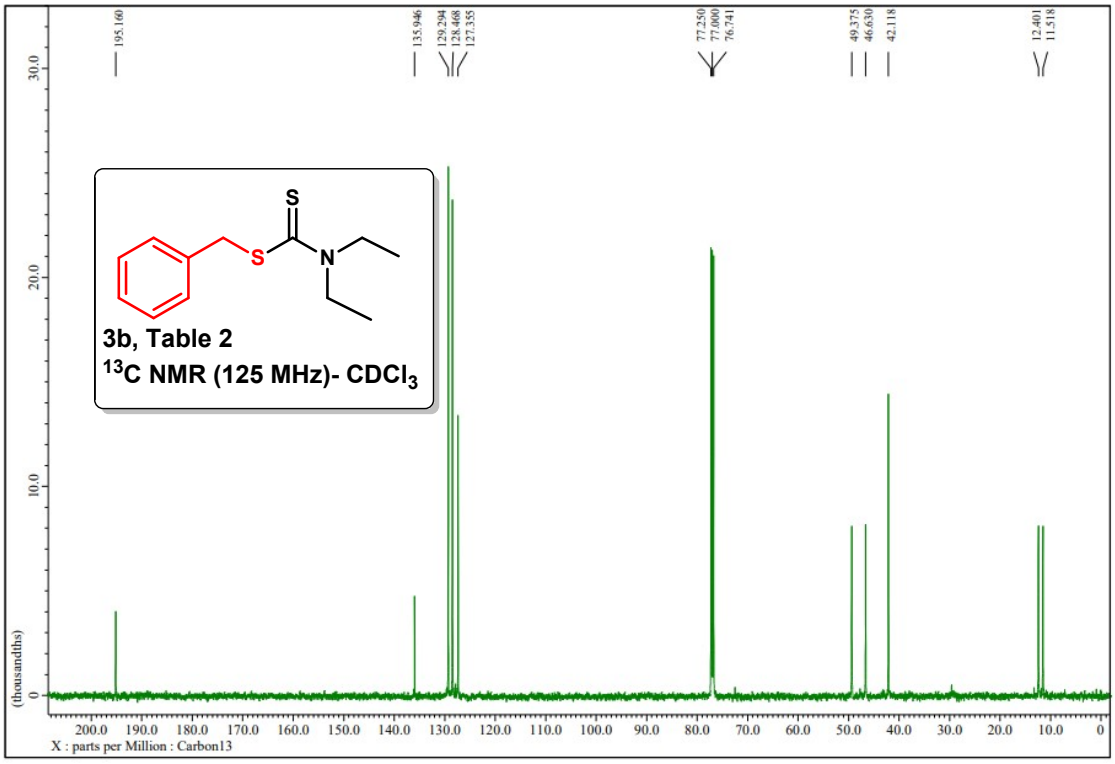
3b, Table 2
13C NMR (125 MHz)- CDCl3
X : parts per Million : Carbon13

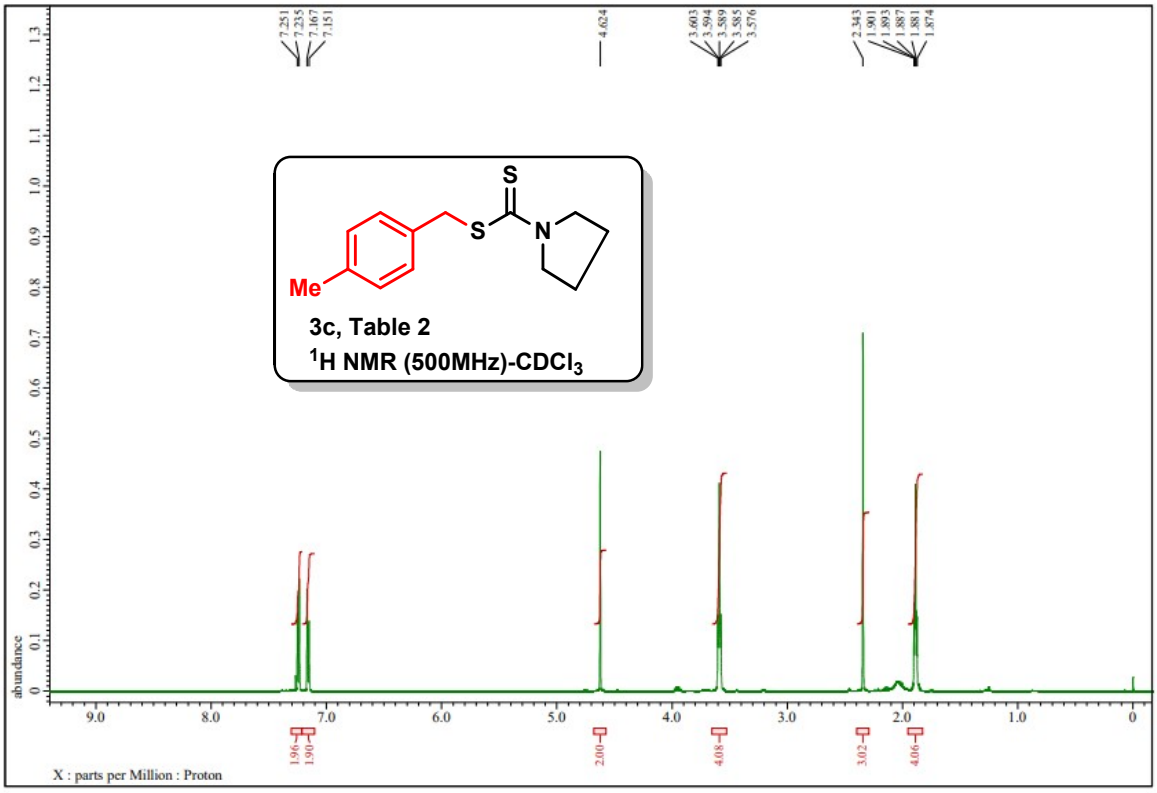
Me
3c, Table 2
1H NMR (500MHz)-CDCl3
X : parts per Million : Proton

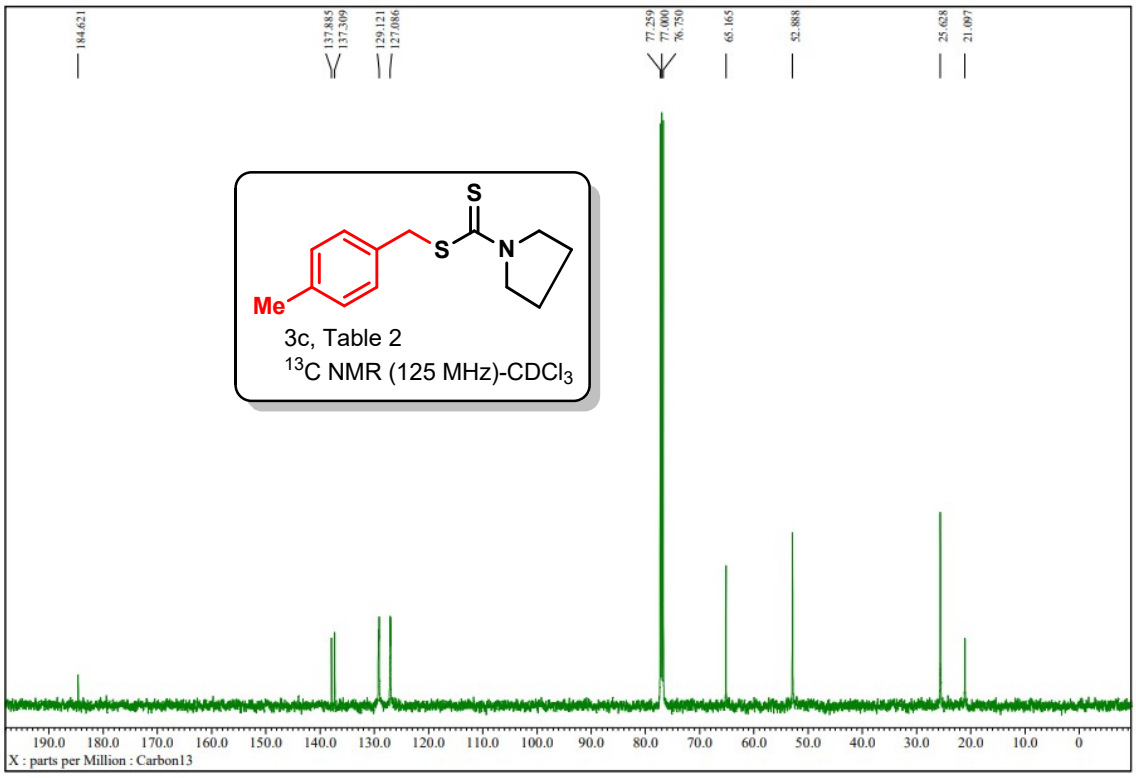
Me
3c, Table 2
13C NMR (125 MHz)-CDCl3
X : parts per Million : Carbon13

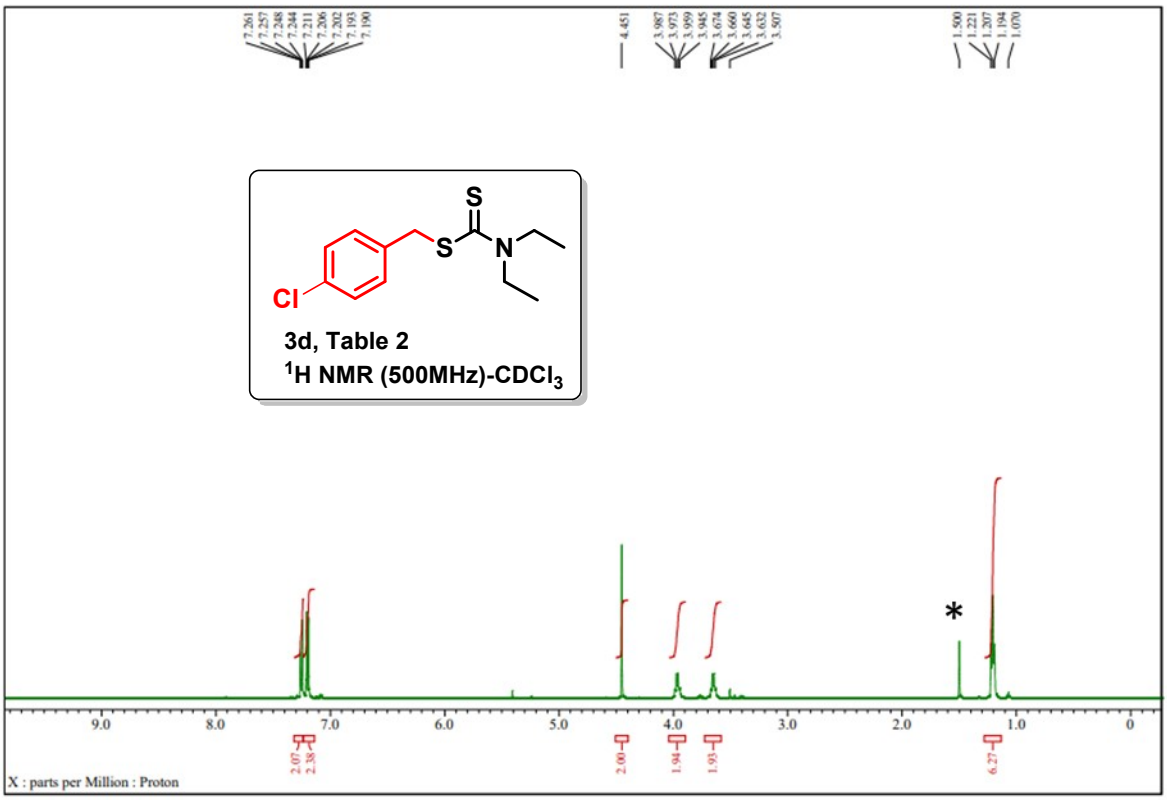
3d, Table 2
1H NMR (500MHz)-CDCl3
X : parts per Million : Proton

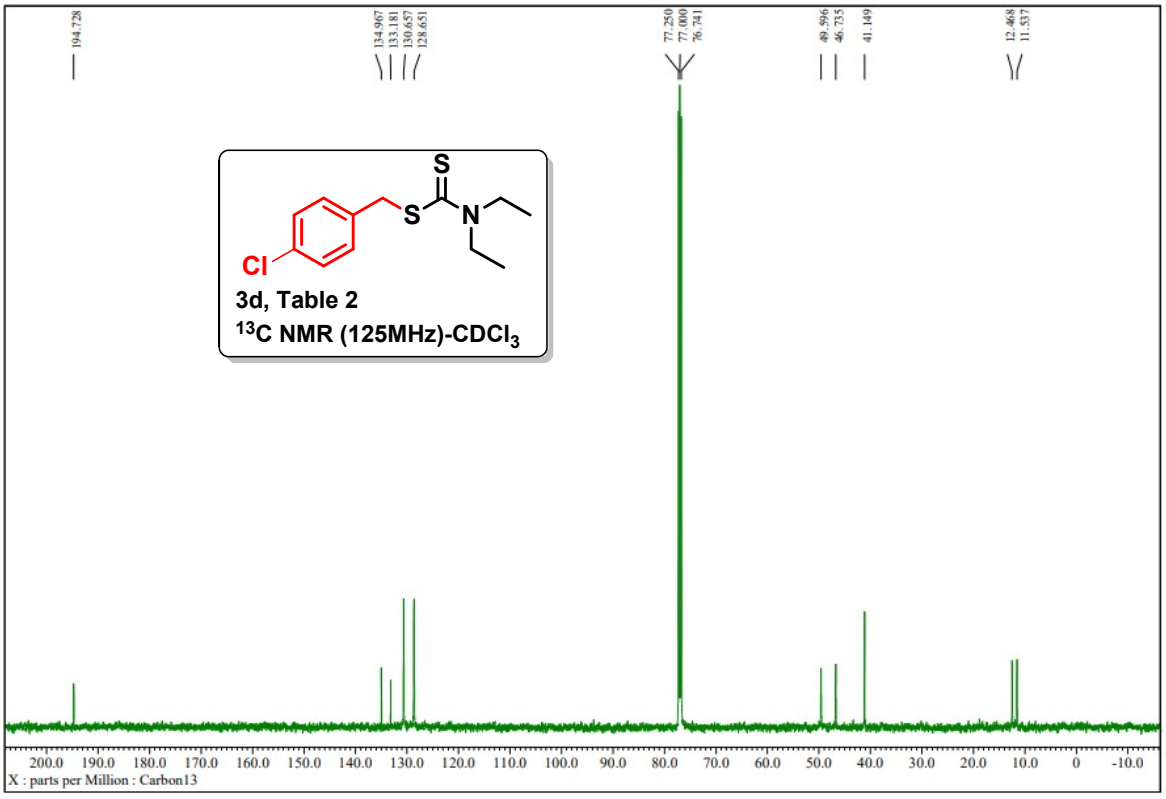
3d, Table 2
13C NMR (125MHz)-CDCl3
X : parts per Million : Carbon13

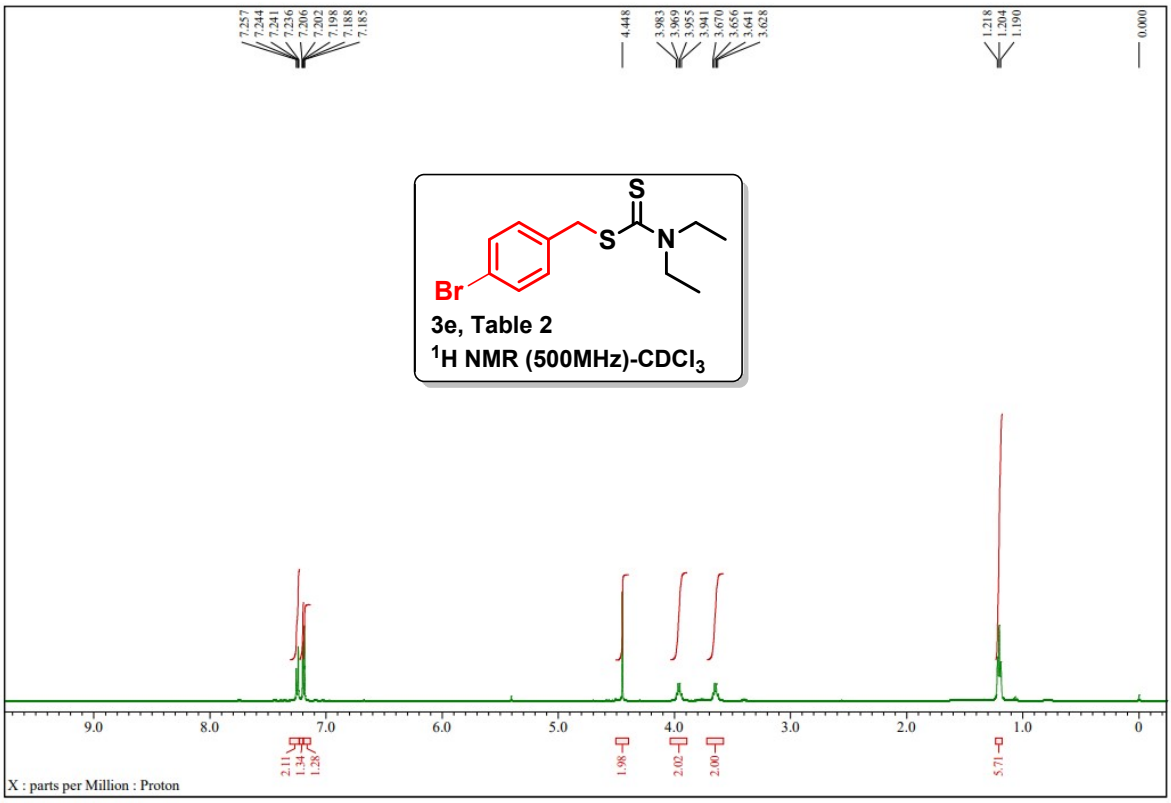
3e, Table 2
1H NMR (500MHz)-CDCl3
X : parts per Million : Proton

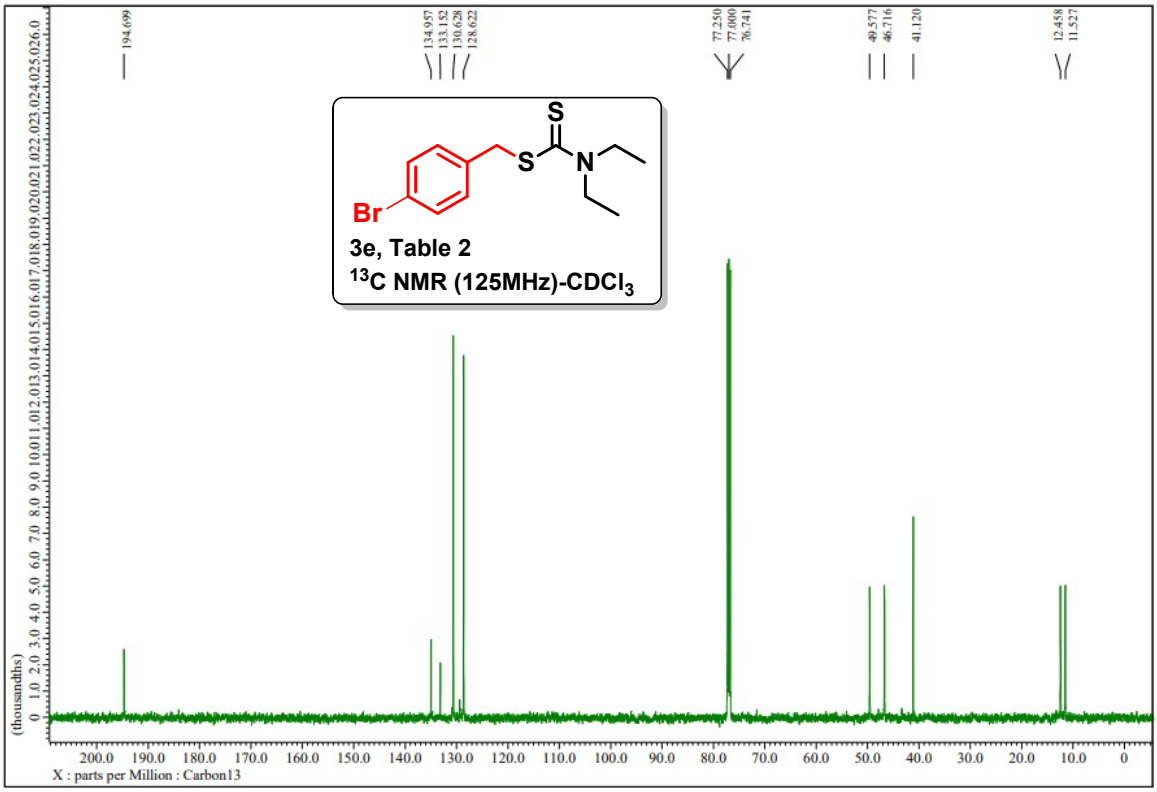
3e, Table 2
13C NMR (125MHz)-CDCl3
X : parts per Million : Carbon13

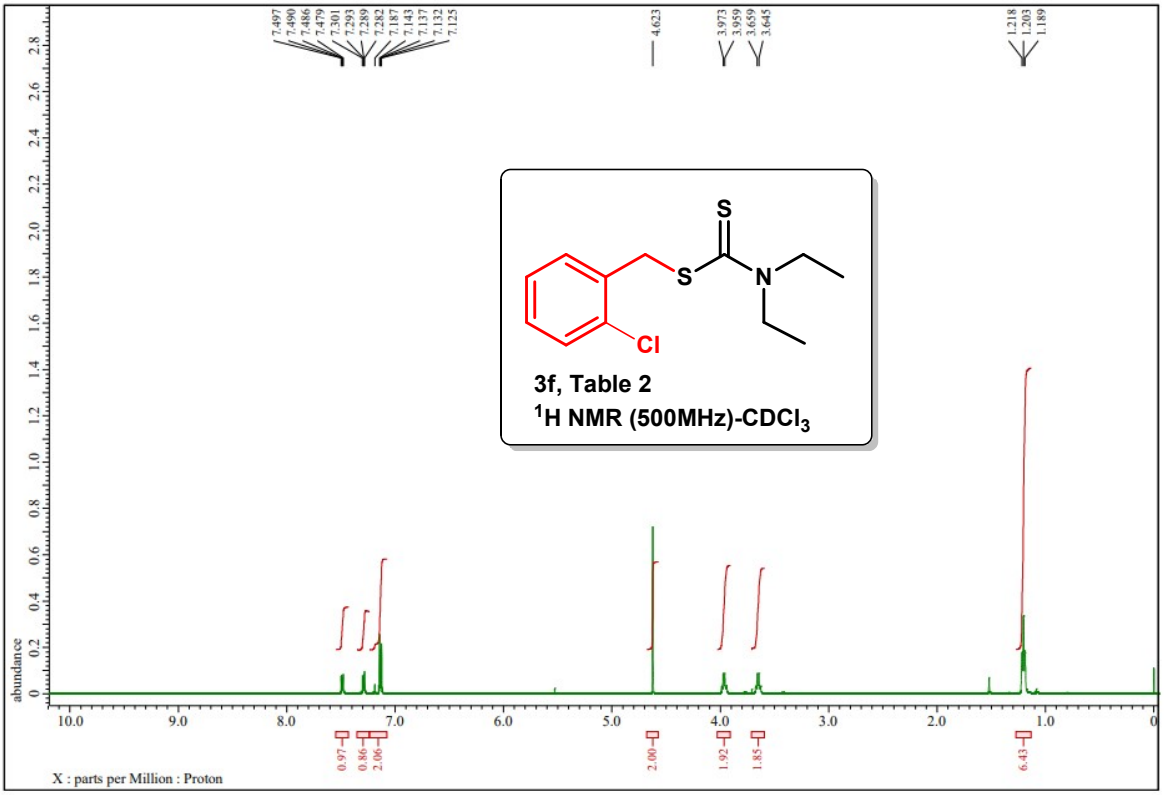
7.497
7.490
7.486
7.479
7.301
7.293
7.289
7.282
7.187
7.143
7.137
7.132
7.125
4.623
3.973
3.959
3.659
3.645
1.218
1.203
1.189
S
S
N
Cl
3f, Table 2
1H NMR (500MHz)-CDCl3
abundance
0.97
0.86
2.06
2.00
1.92
1.85
6.43
X : parts per Million : Proton

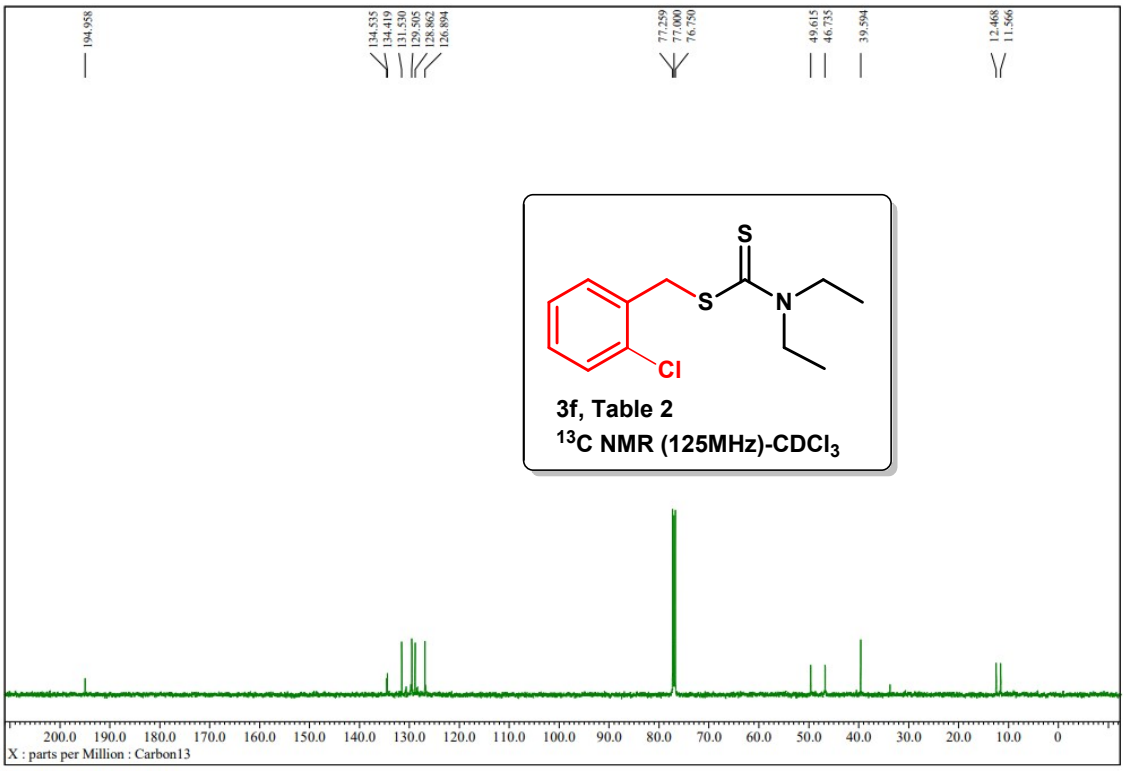
194.958
134.535
134.419
131.530
129.505
128.862
126.894
77.259
77.000
76.750
49.615
46.735
39.594
12.468
11.566
S
S
N
Cl
3f, Table 2
13C NMR (125MHz)-CDCl3
X : parts per Million : Carbon13

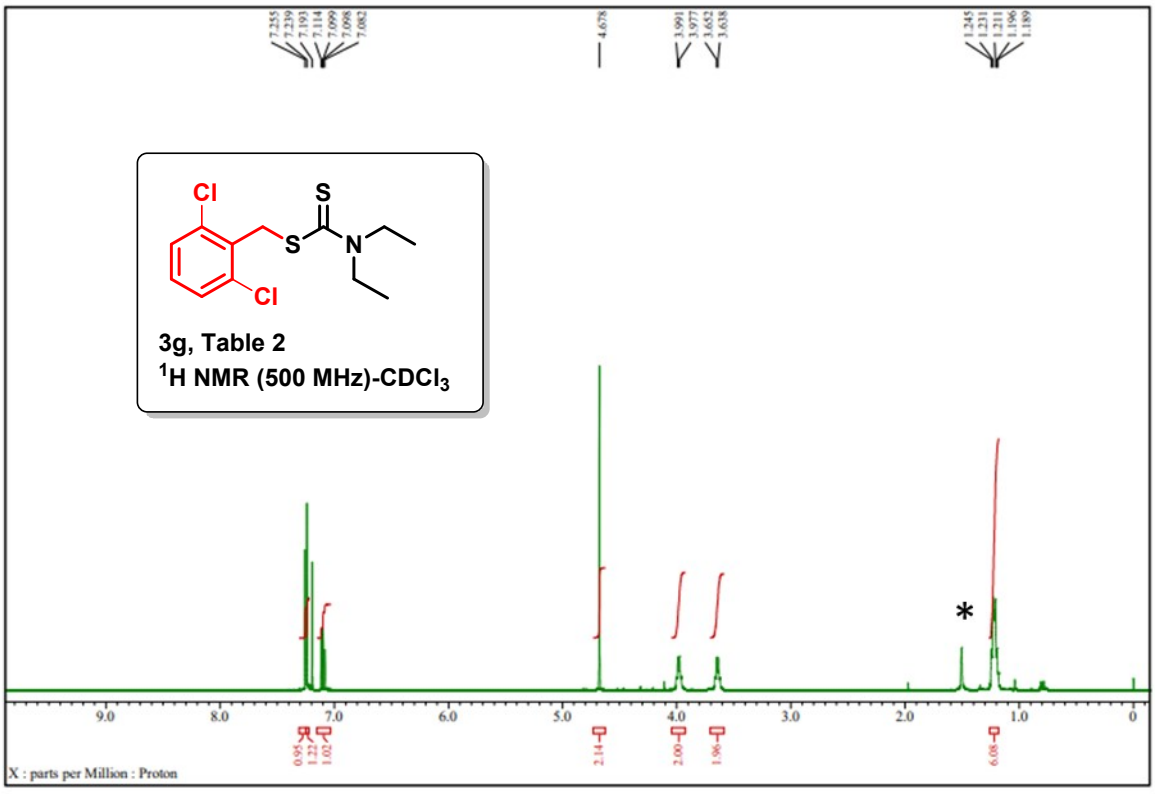
Cl
S
S
N
Cl
3g, Table 2
1H NMR (500 MHz)-CDCl3
*
X : parts per Million : Proton

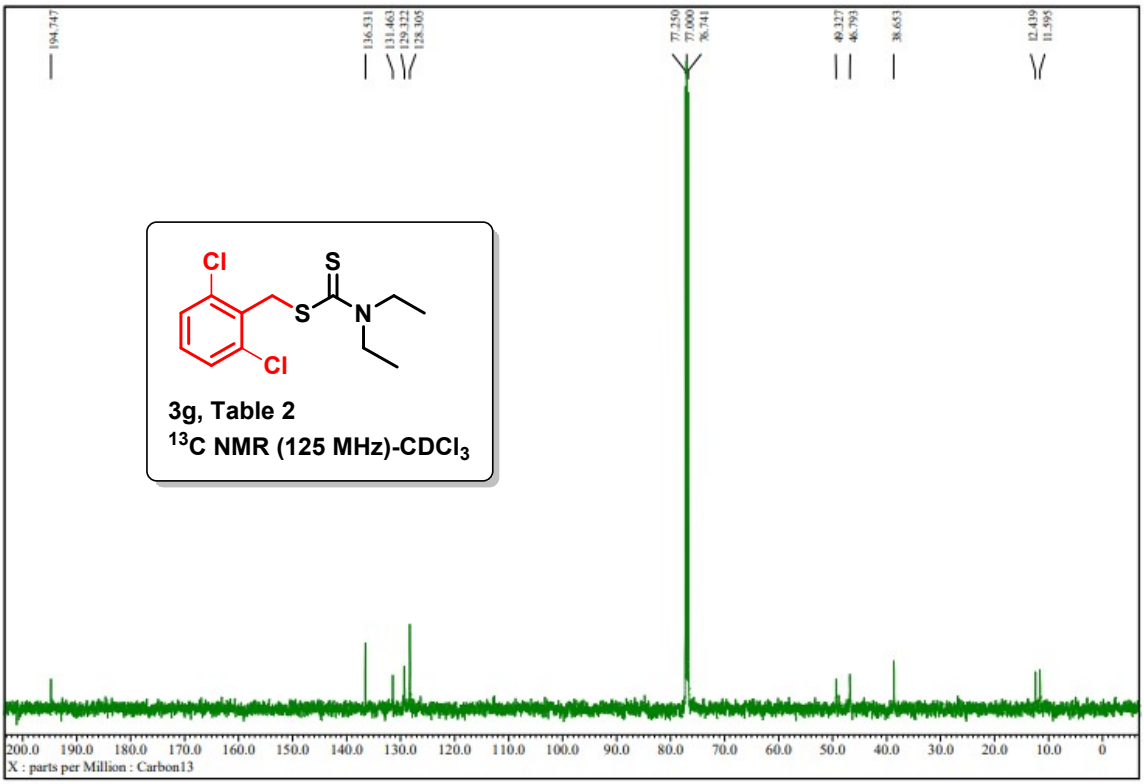
Cl
S
S
N
Cl
3g, Table 2
13C NMR (125 MHz)-CDCl3
X : parts per Million : Carbon13

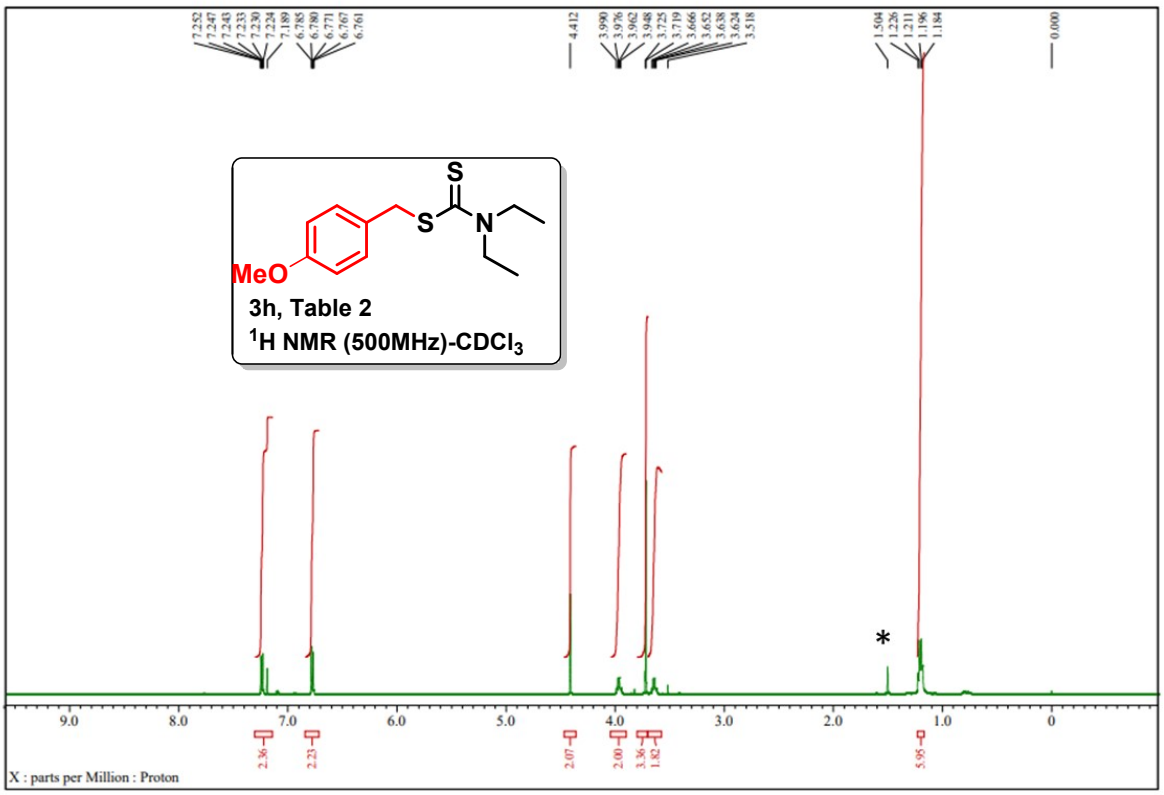
MeO
3h, Table 2
^{1}H NMR (500MHz)-CDCl$_3$
X : parts per Million : Proton

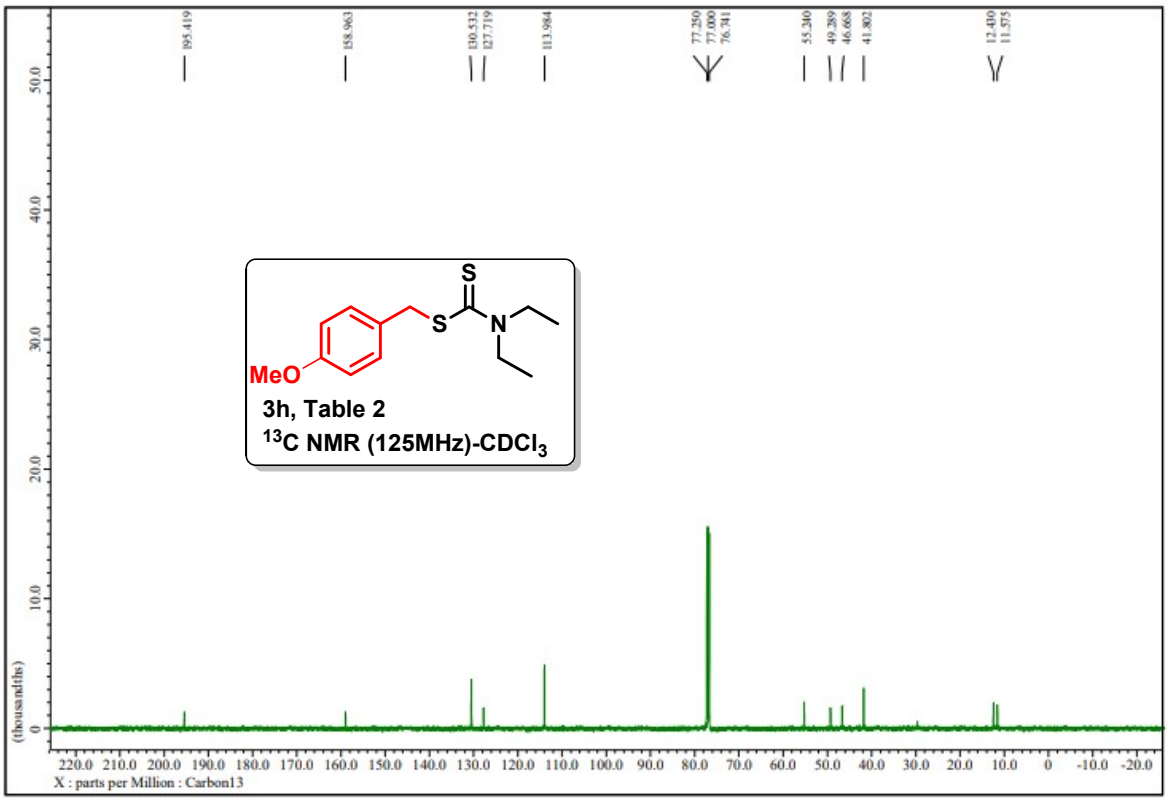
MeO
3h, Table 2
^{13}C NMR (125MHz)-CDCl$_3$
X : parts per Million : Carbon13

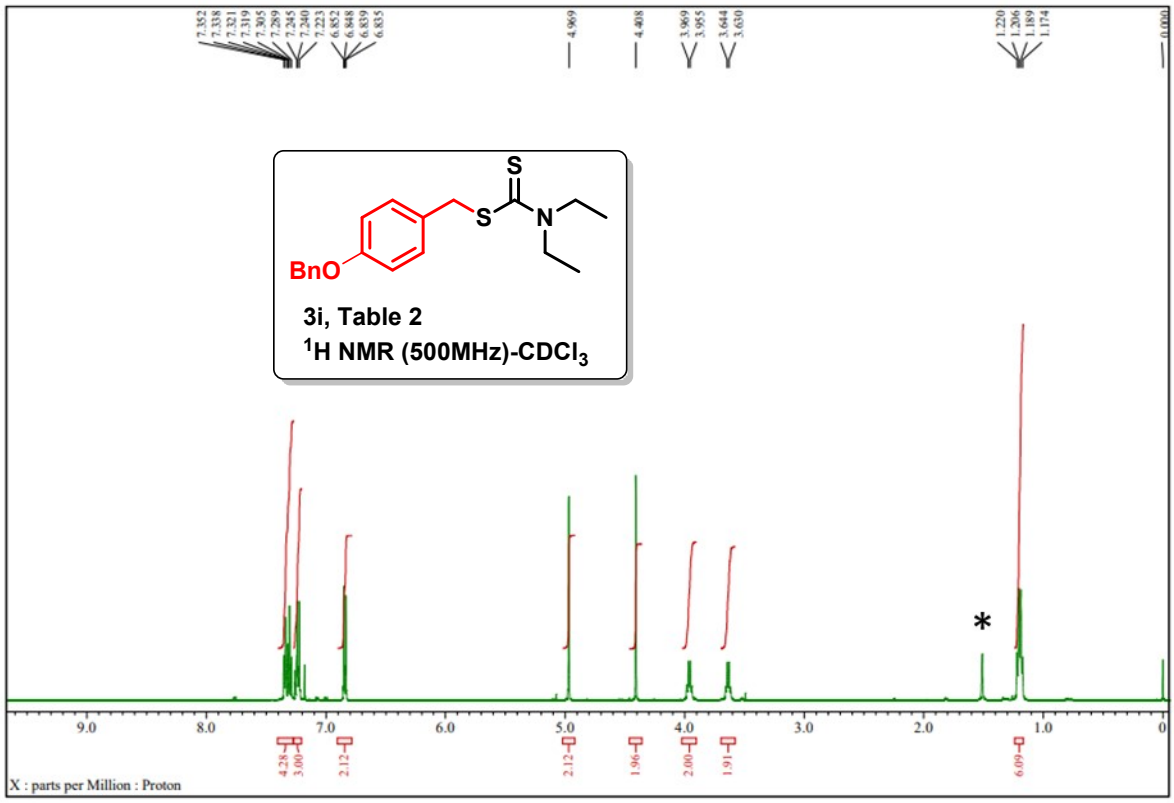
BnO
S
S
N
3i, Table 2
1H NMR (500MHz)-CDCl3
*
X : parts per Million : Proton

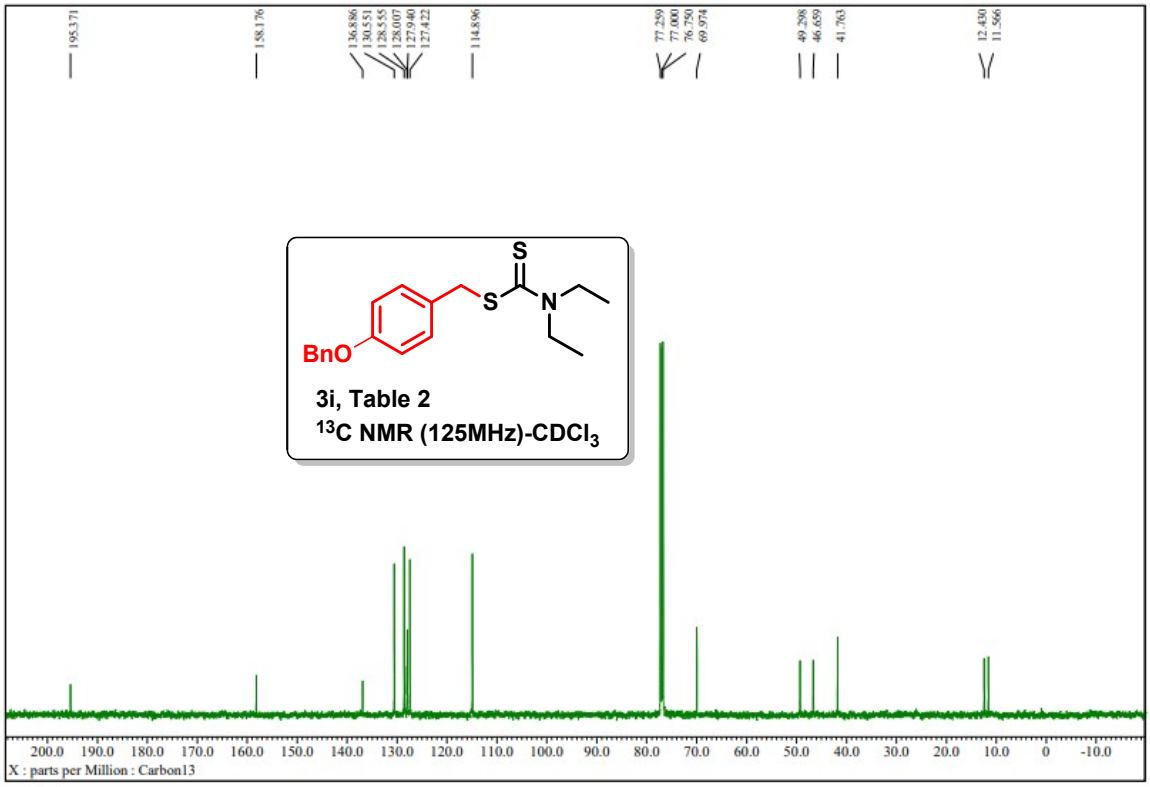
BnO
S
S
N
3i, Table 2
13C NMR (125MHz)-CDCl3
X : parts per Million : Carbon13

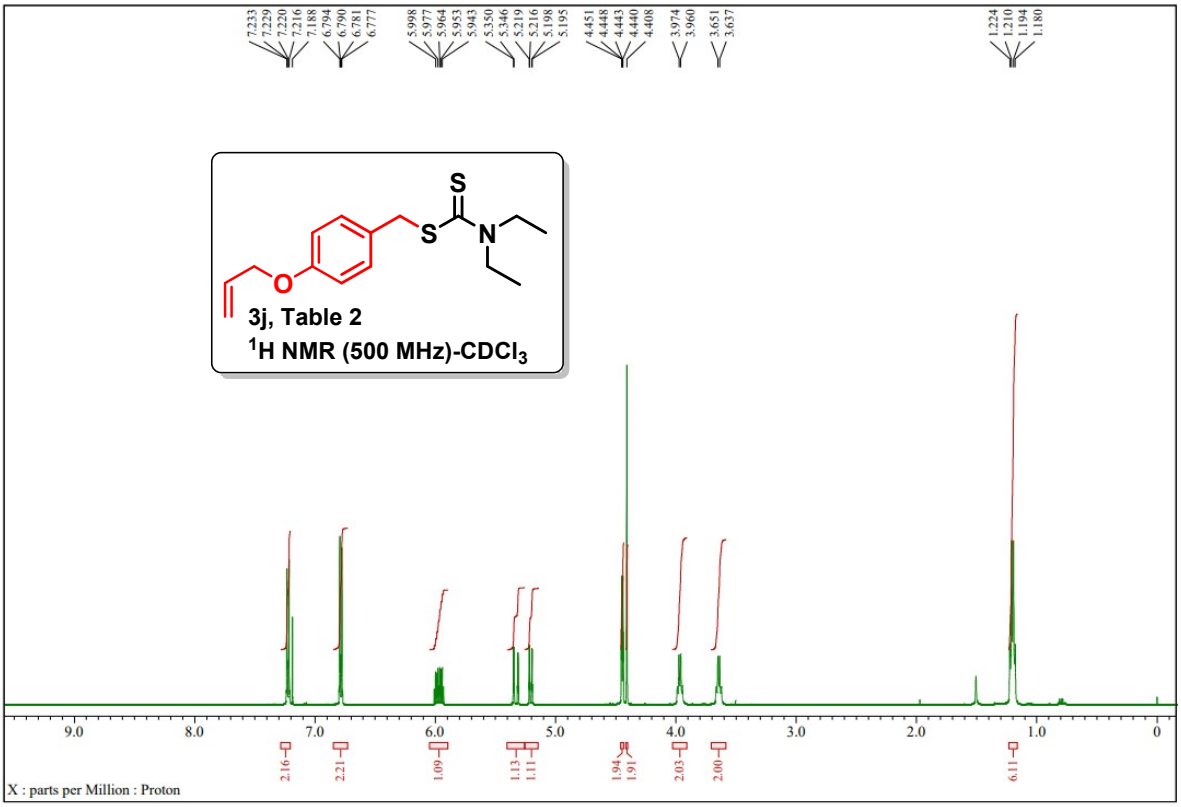
3j, Table 2
^{1}H NMR (500 MHz)-CDCl$_3$
X : parts per Million : Proton

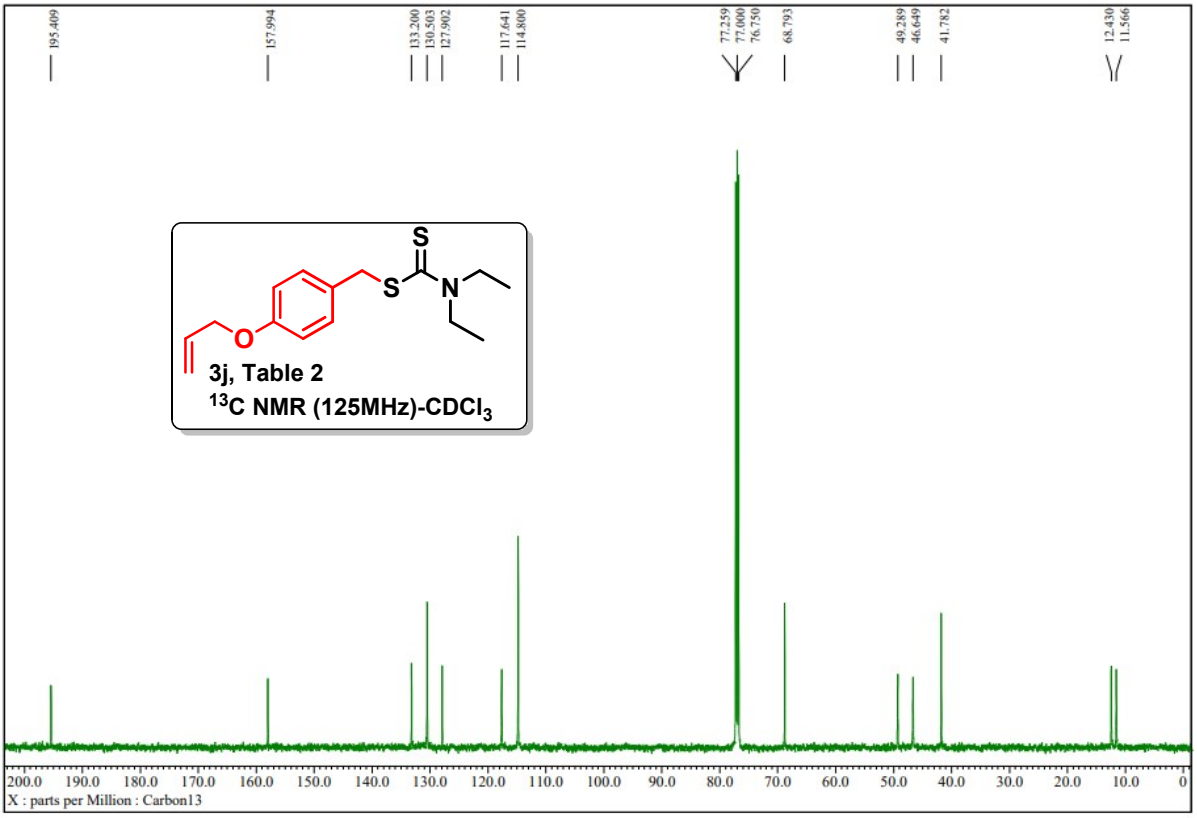
3j, Table 2
^{13}C NMR (125MHz)-CDCl$_3$
X : parts per Million : Carbon13

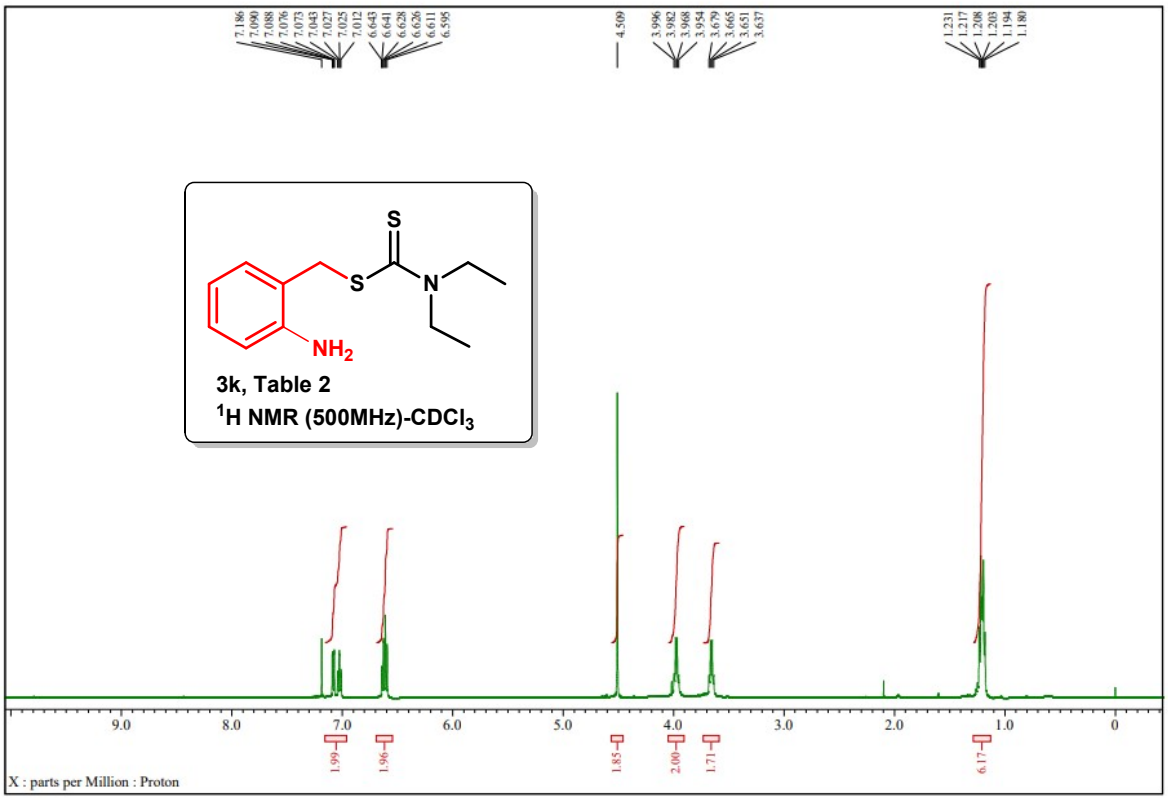
3k, Table 2
^{1}H NMR (500MHz)-CDCl$_3$
X : parts per Million : Proton

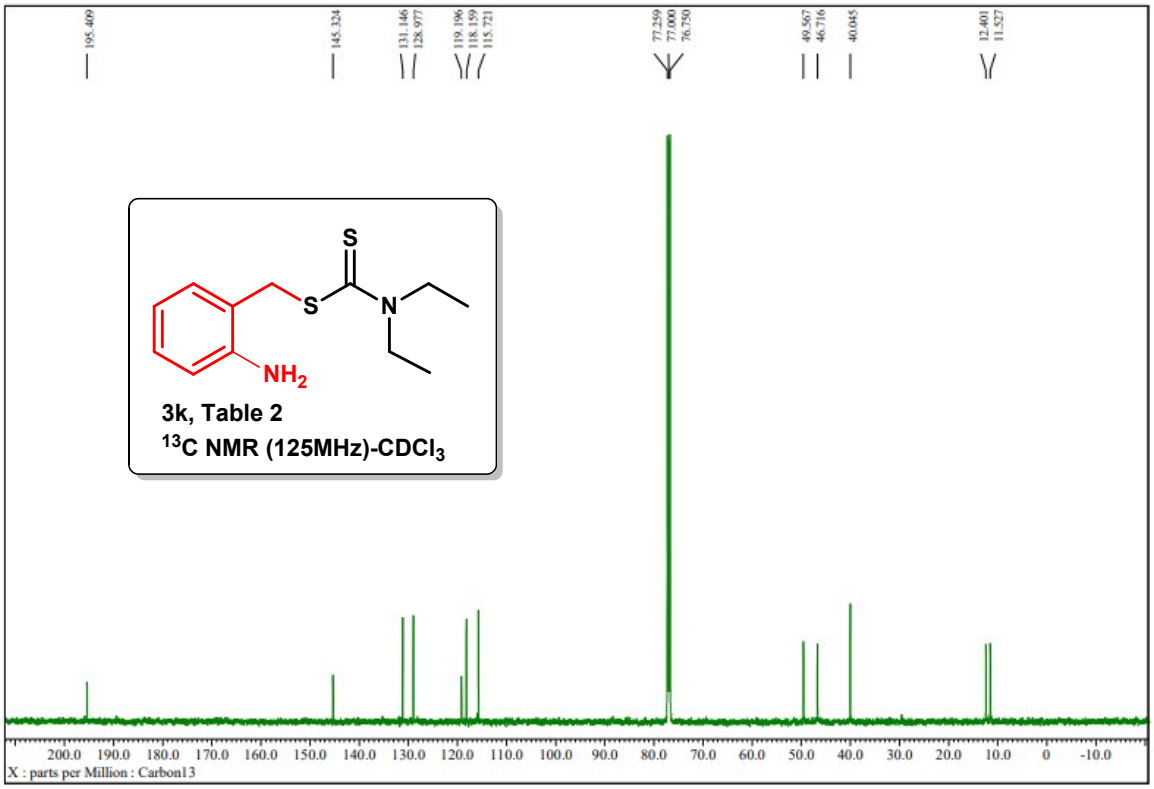
3k, Table 2
^{13}C NMR (125MHz)-CDCl$_3$
X : parts per Million : Carbon13

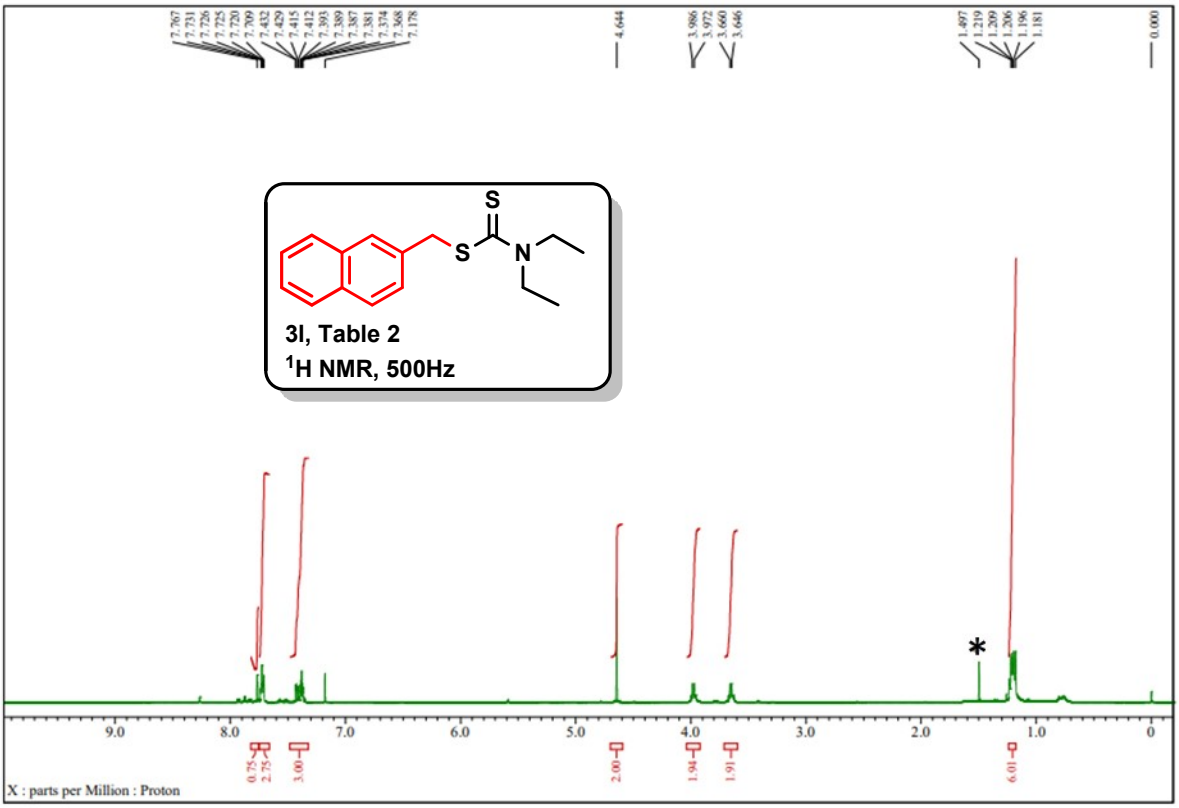
3l, Table 2
1H NMR, 500Hz
X : parts per Million : Proton

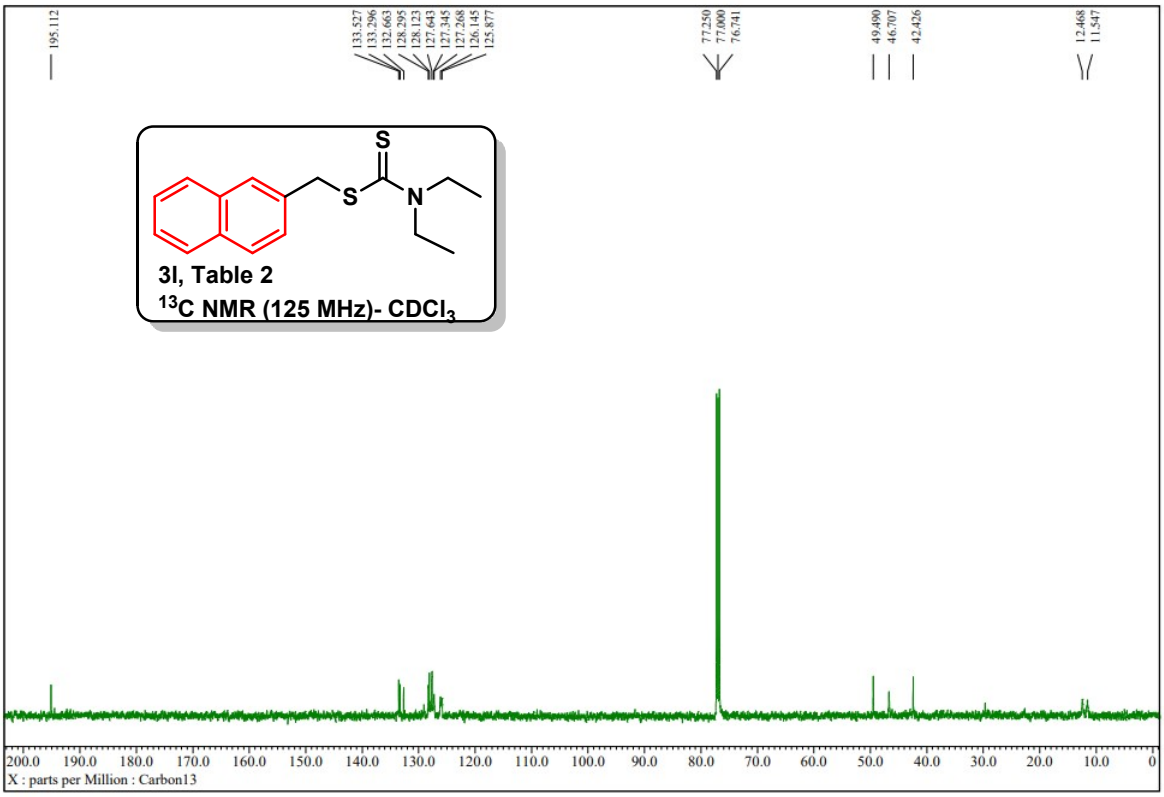
3l, Table 2
13C NMR (125 MHz)- CDCl3
X : parts per Million : Carbon13

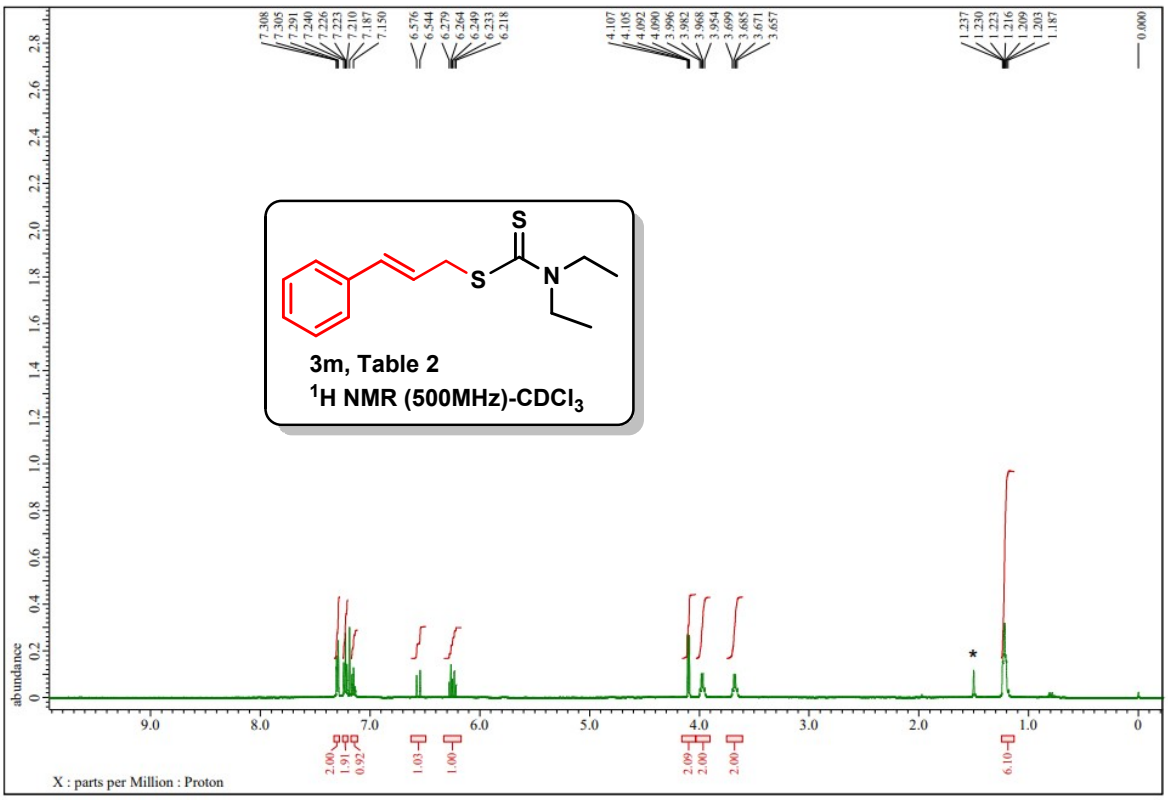
3m, Table 2
1H NMR (500MHz)-CDCl3
abundance
X : parts per Million : Proton

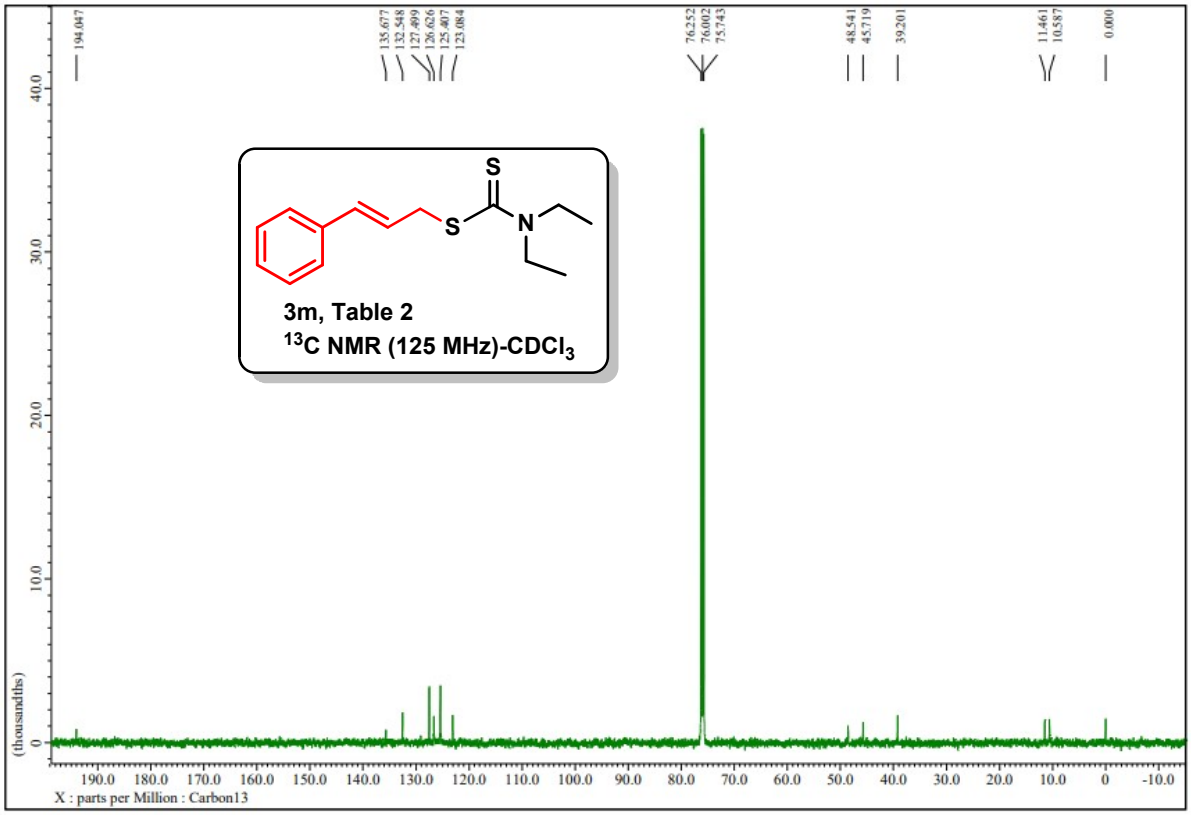
3m, Table 2
13C NMR (125 MHz)-CDCl3
(thousandths)
X : parts per Million : Carbon13

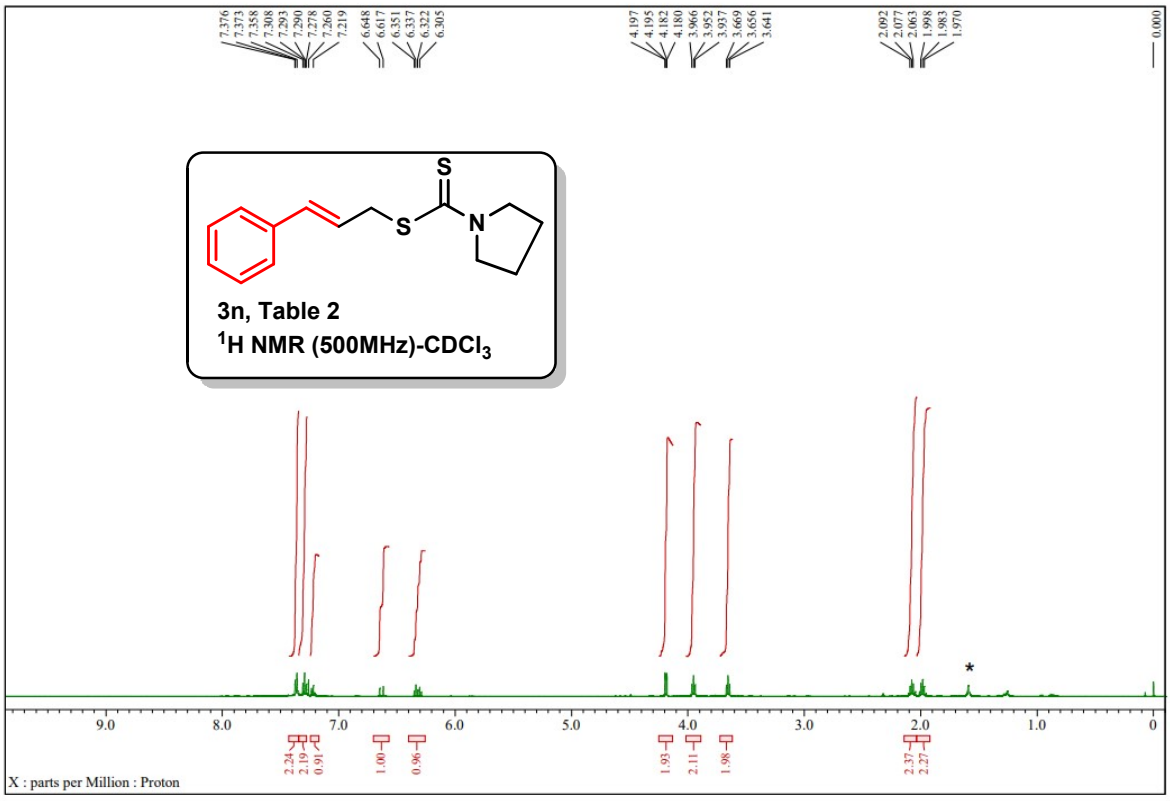
3n, Table 2
1H NMR (500MHz)-CDCl3
X : parts per Million : Proton

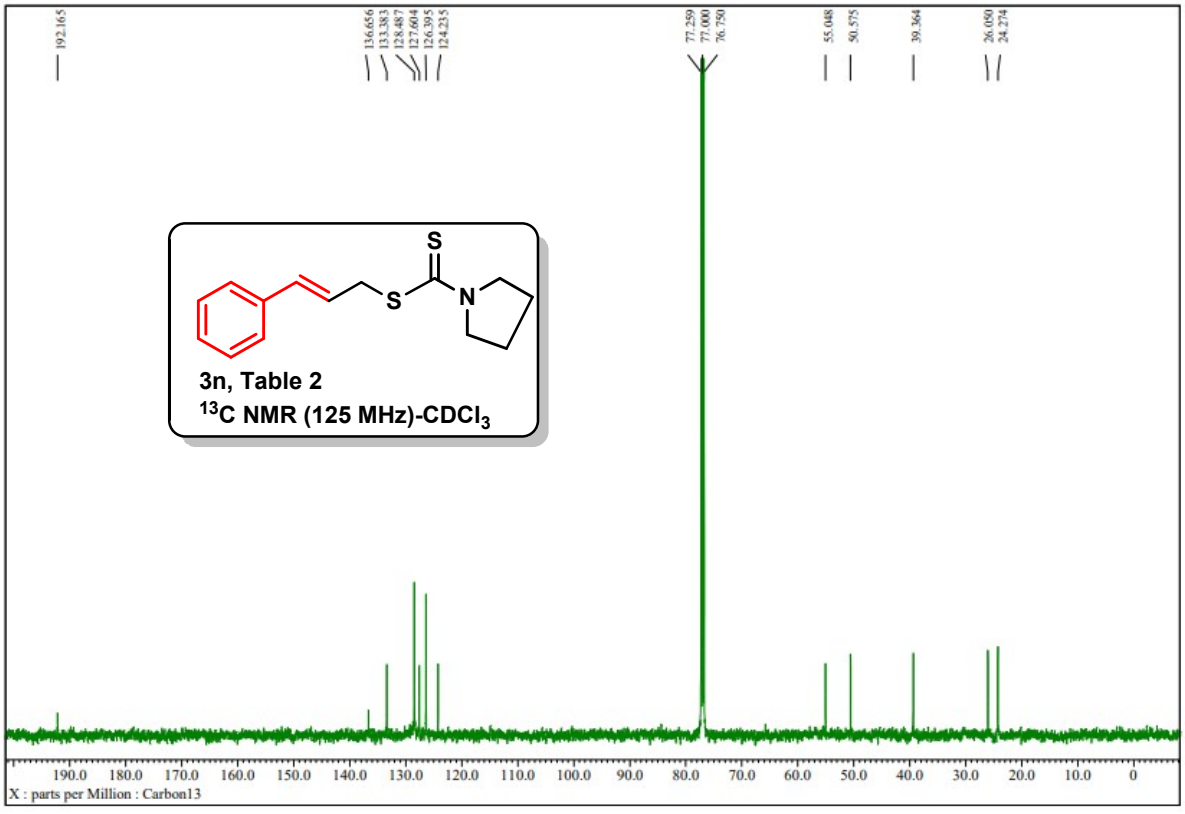
3n, Table 2
13C NMR (125 MHz)-CDCl3
X : parts per Million : Carbon13

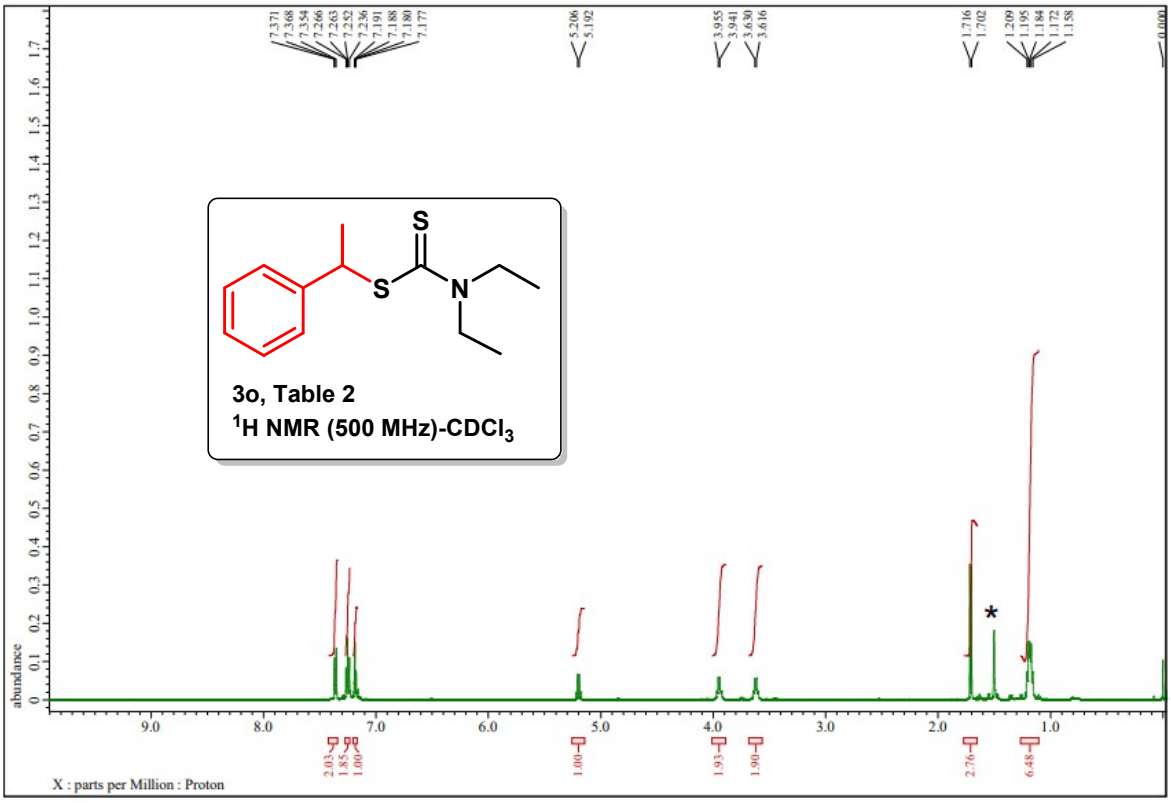
3o, Table 2
^{1}H NMR (500 MHz)-CDCl$_3$
X : parts per Million : Proton

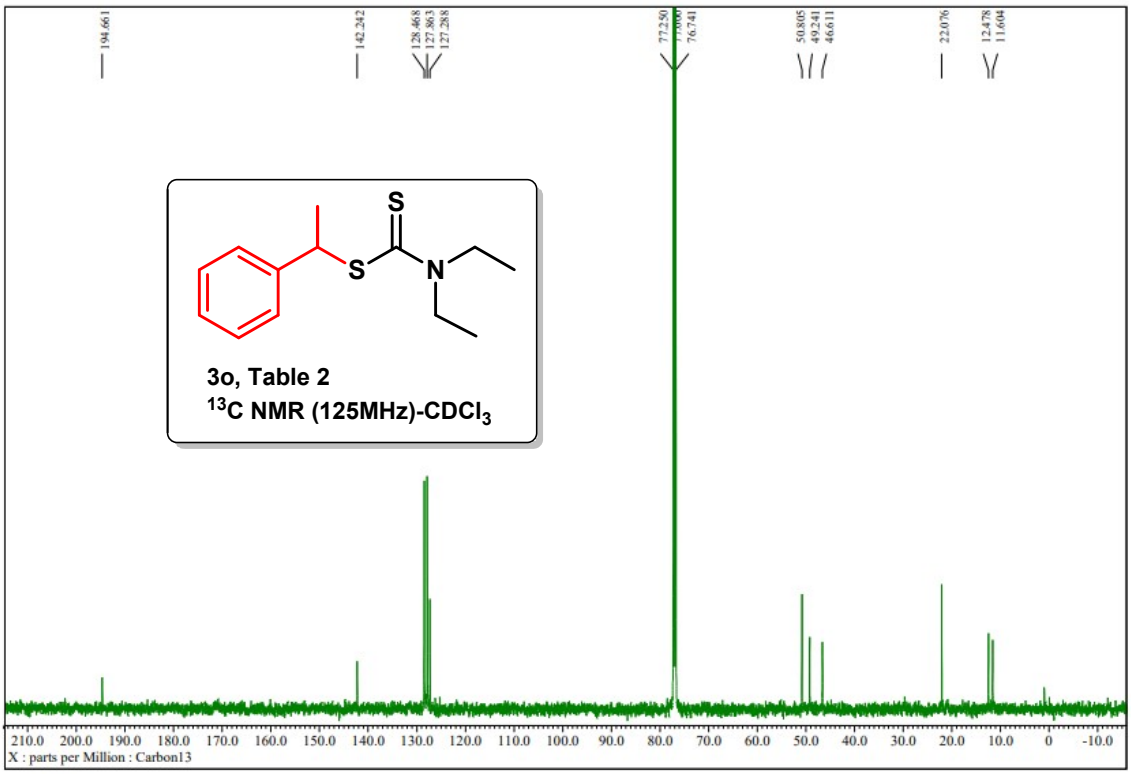
3o, Table 2
^{13}C NMR (125MHz)-CDCl$_3$
X : parts per Million : Carbon13

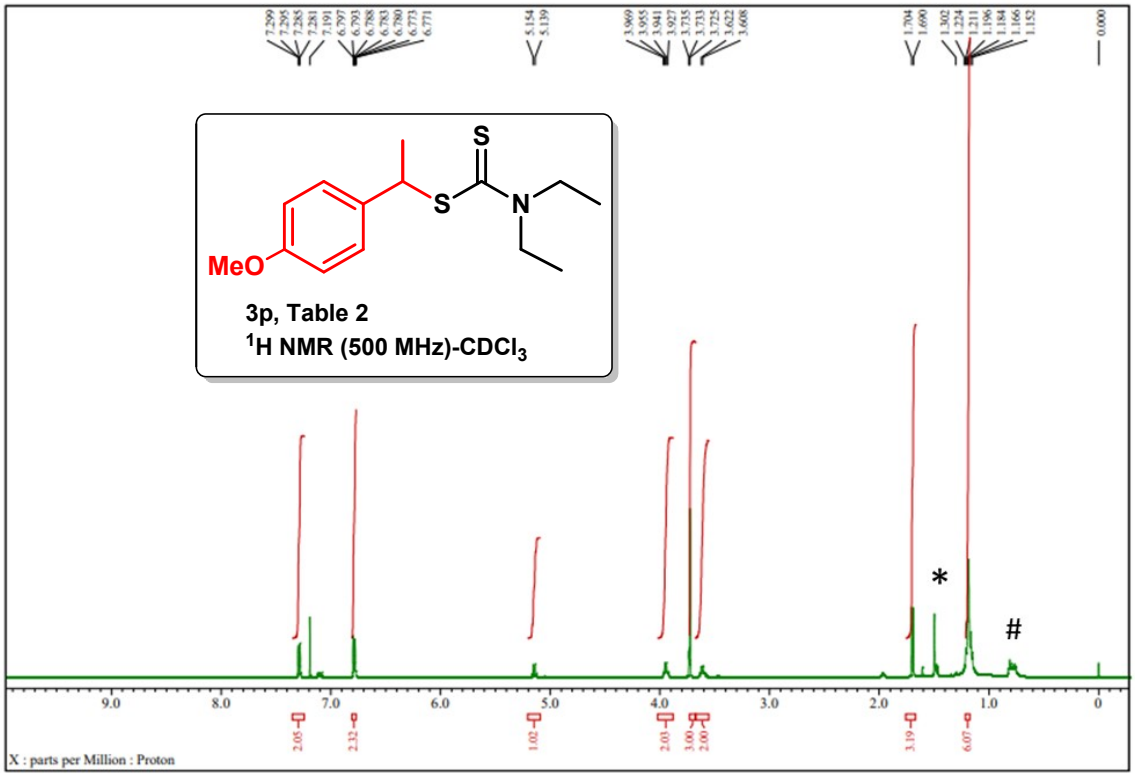
MeO
S
S
N
3p, Table 2
1H NMR (500 MHz)-CDCl3
*
#
X : parts per Million : Proton

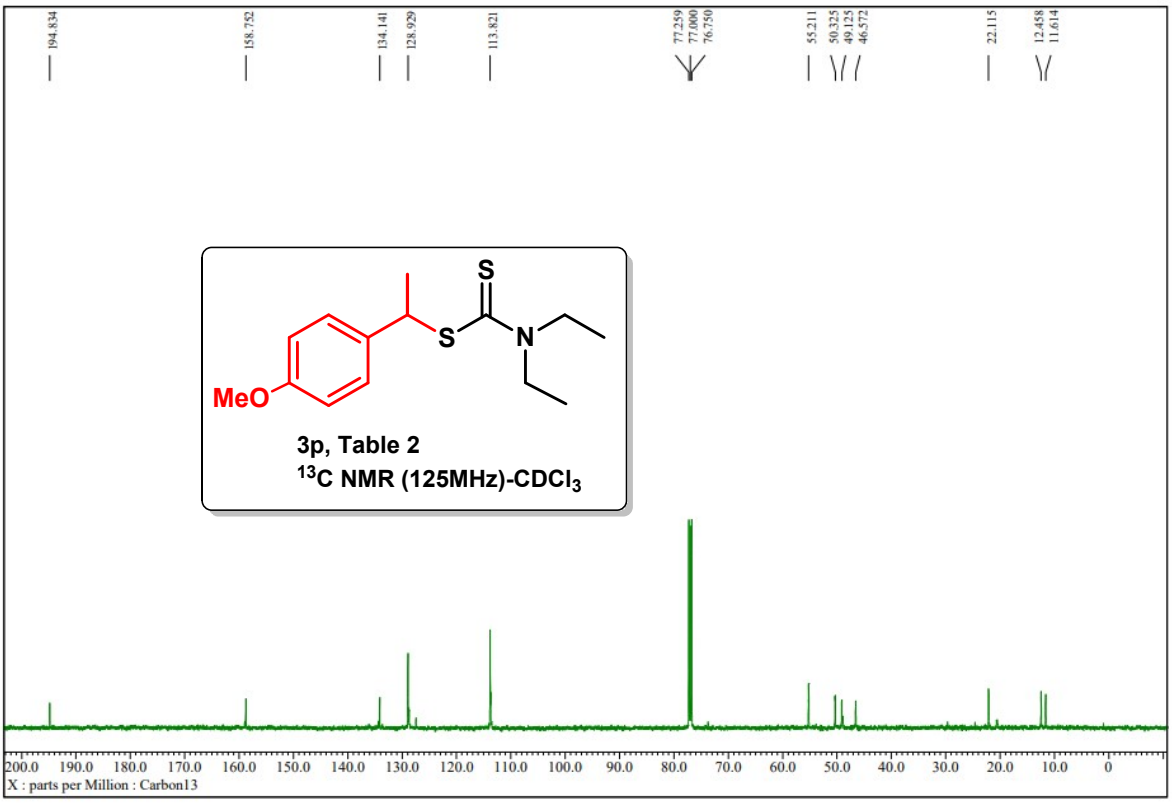
MeO
S
S
N
3p, Table 2
13C NMR (125MHz)-CDCl3
X : parts per Million : Carbon13

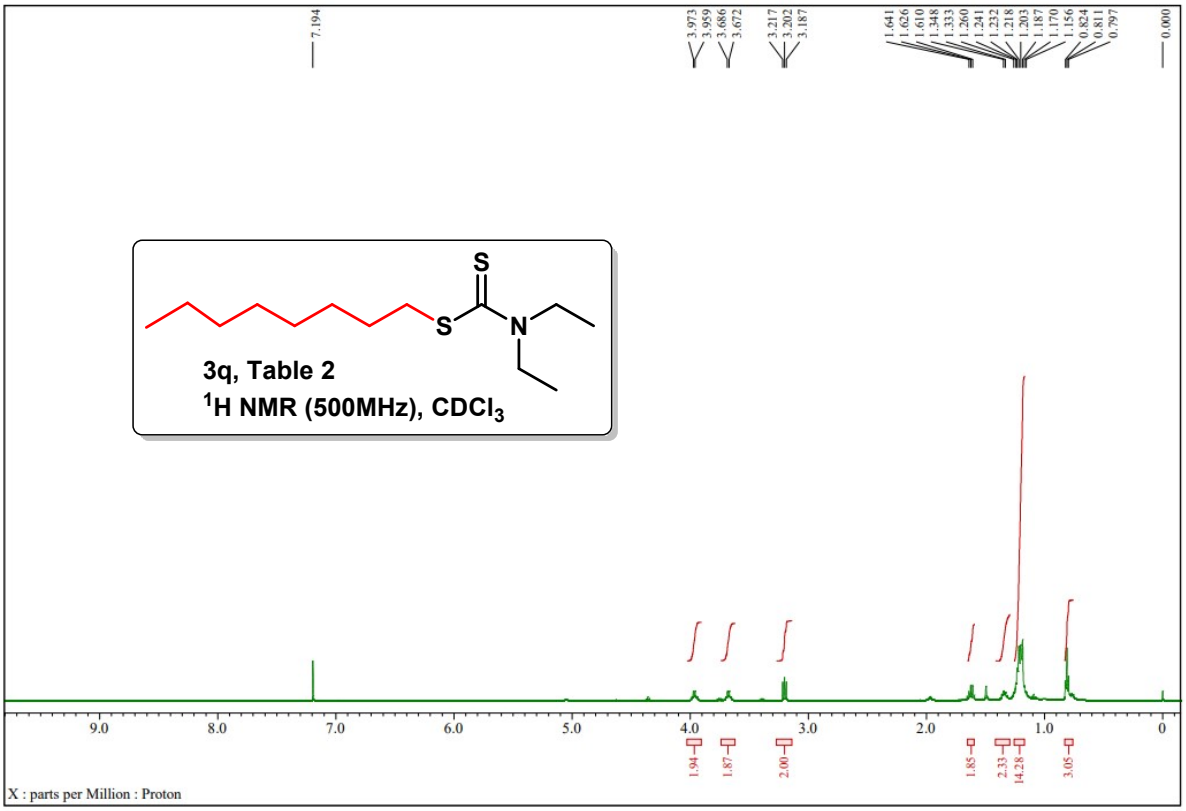
3q, Table 2
1H NMR (500MHz), CDCl3
X : parts per Million : Proton

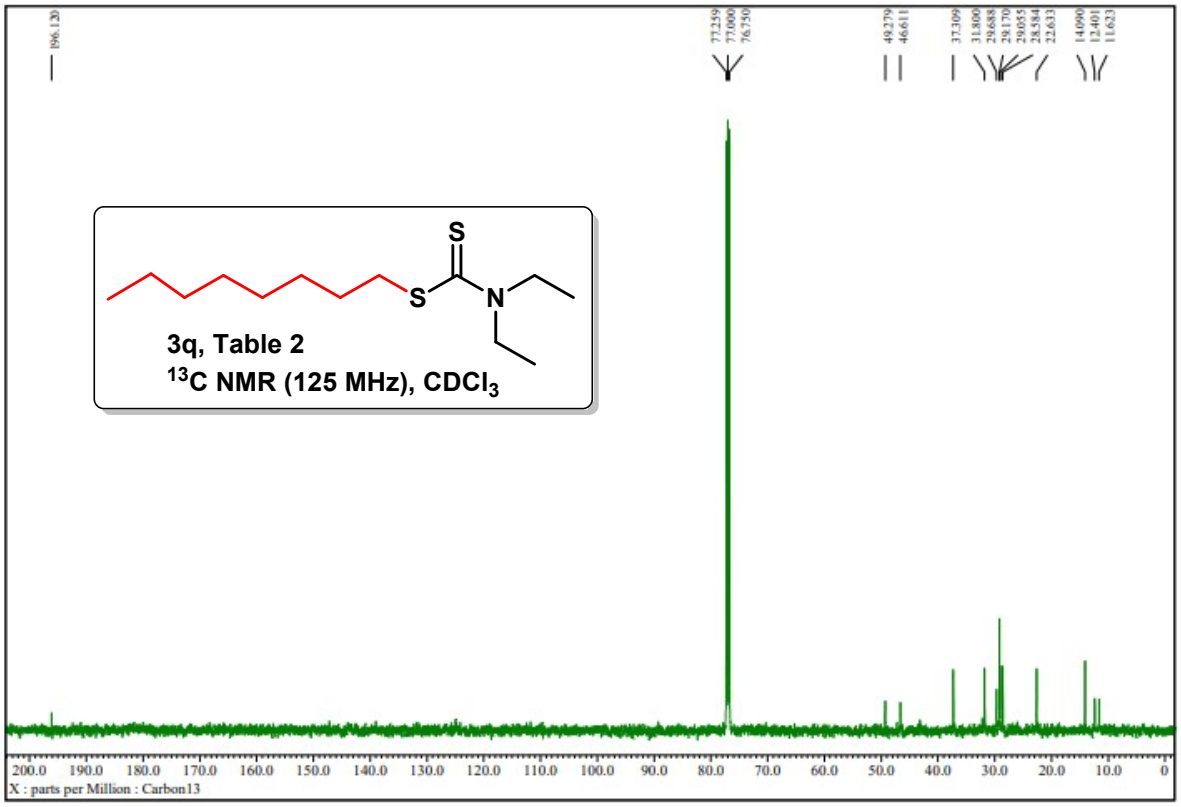
3q, Table 2
13C NMR (125 MHz), CDCl3
X : parts per Million : Carbon13

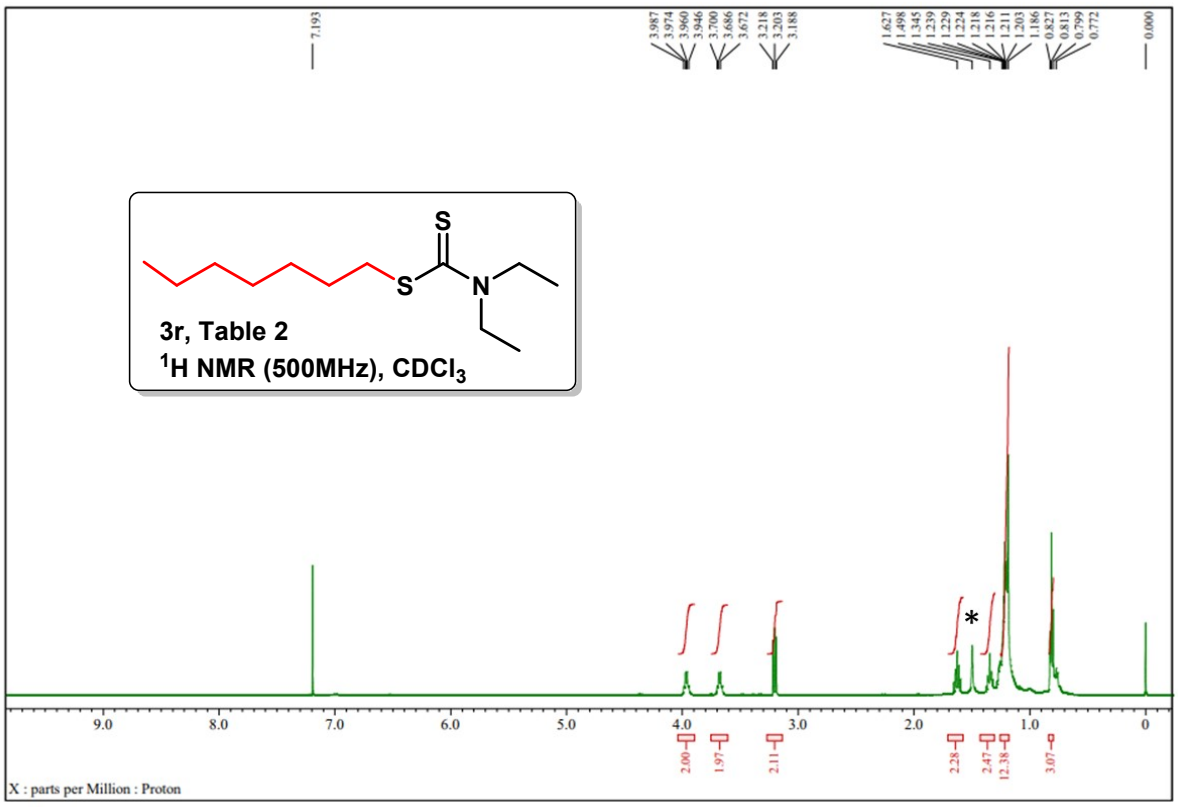
3r, Table 2
1H NMR (500MHz), CDCl3
X : parts per Million : Proton

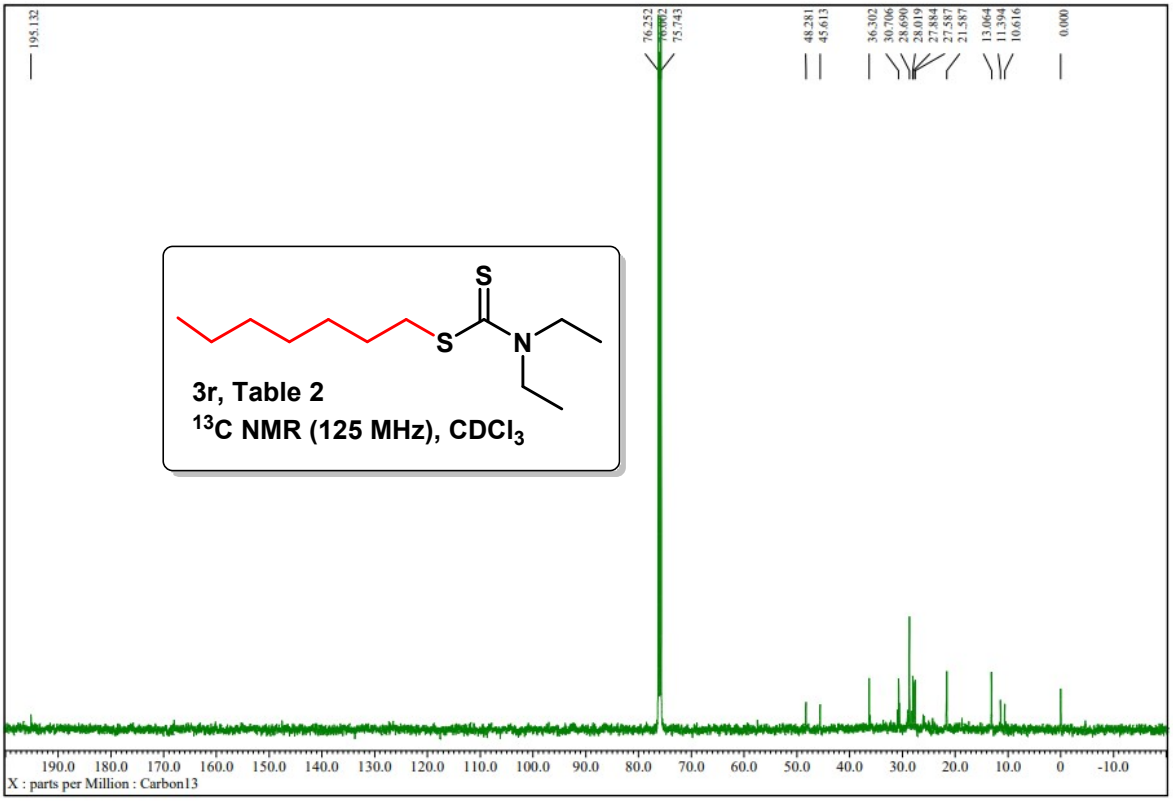
3r, Table 2
13C NMR (125 MHz), CDCl3
X : parts per Million : Carbon13

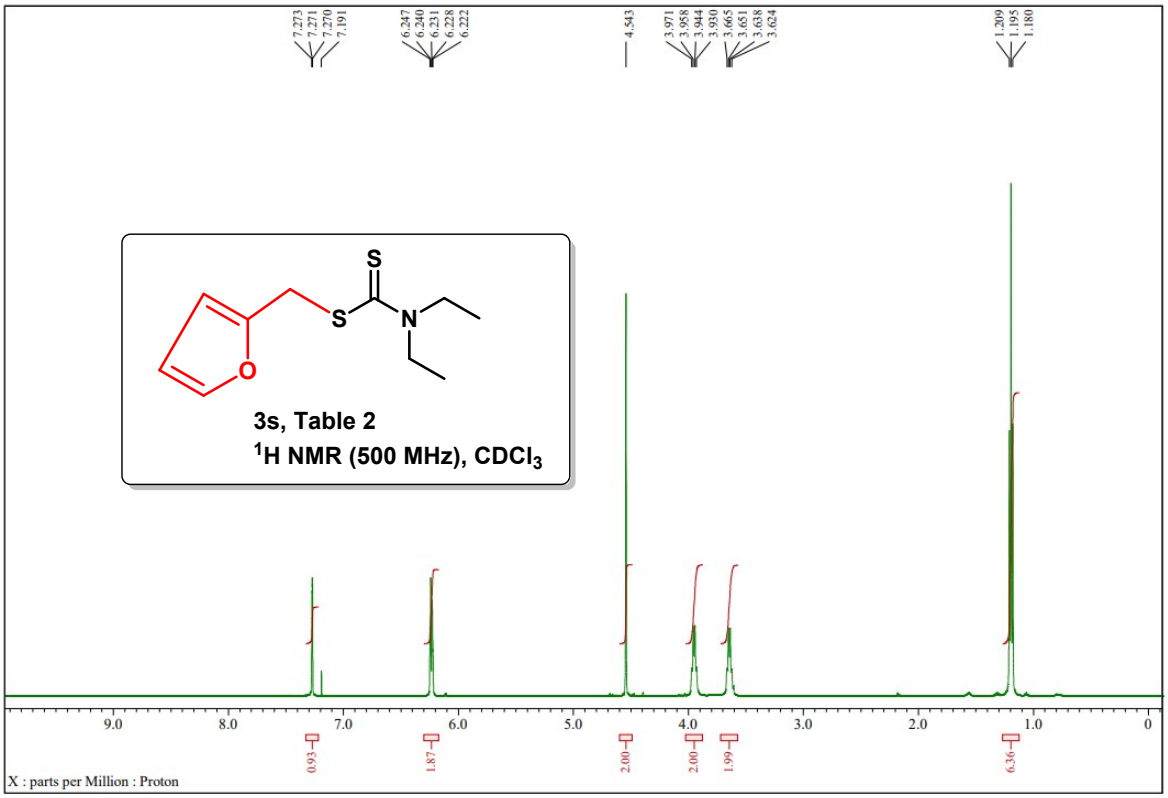
7.273
7.271
7.270
7.191
6.247
6.240
6.231
6.228
6.222
4.543
3.971
3.958
3.944
3.930
3.665
3.651
3.638
3.624
1.209
1.195
1.180
S
S
N
O
3s, Table 2
1H NMR (500 MHz), CDCl3
9.0
8.0
7.0
6.0
5.0
4.0
3.0
2.0
1.0
0
0.93
1.87
2.00
2.00
1.99
6.36
X : parts per Million : Proton

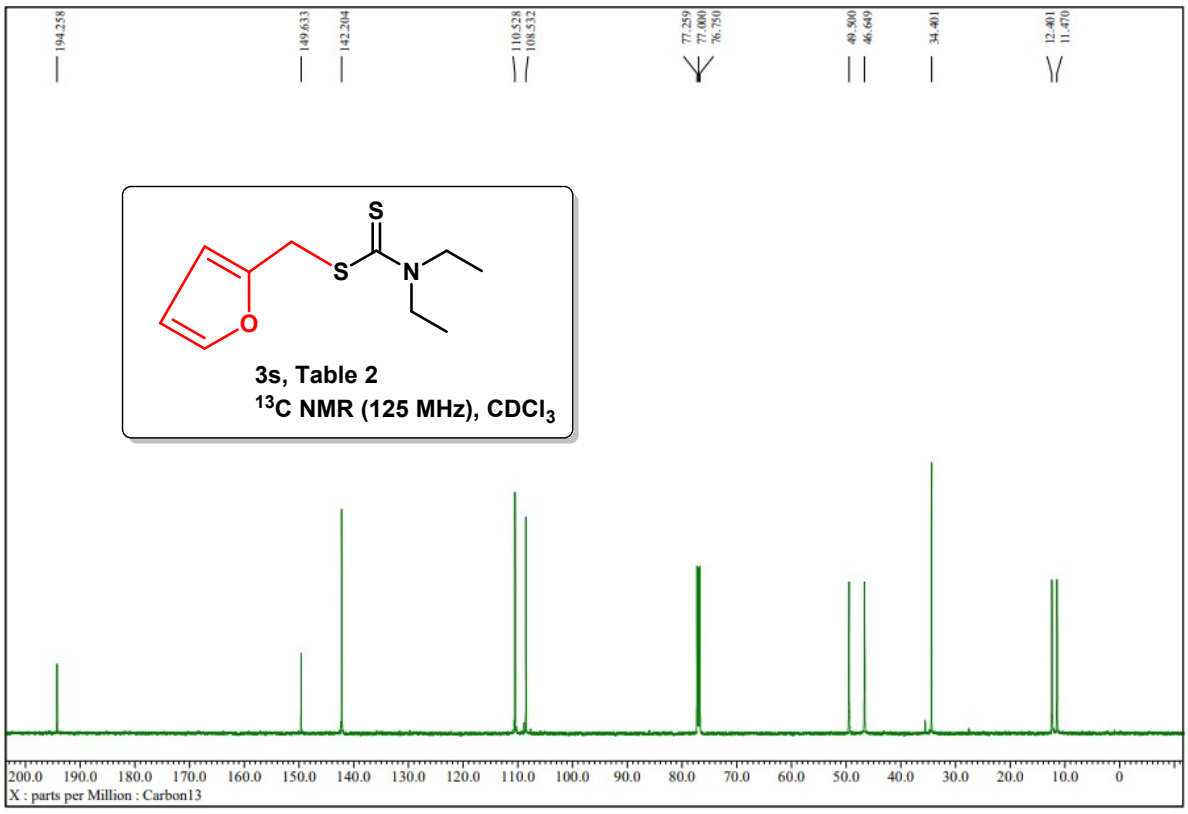
194.258
149.633
142.204
110.528
108.532
77.259
77.000
76.750
49.500
46.649
34.401
12.401
11.470
S
S
N
O
3s, Table 2
13C NMR (125 MHz), CDCl3
200.0
190.0
180.0
170.0
160.0
150.0
140.0
130.0
120.0
110.0
100.0
90.0
80.0
70.0
60.0
50.0
40.0
30.0
20.0
10.0
0
X : parts per Million : Carbon13

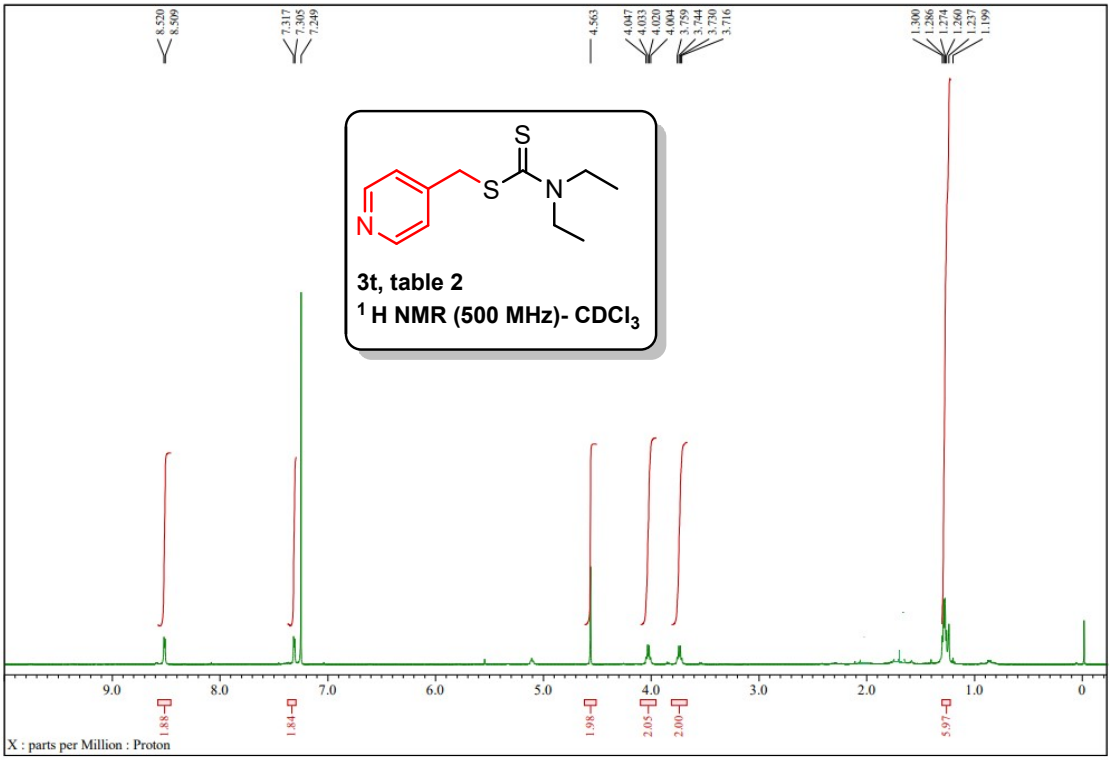
3t, table 2
1 H NMR (500 MHz)- CDCl3
X : parts per Million : Proton

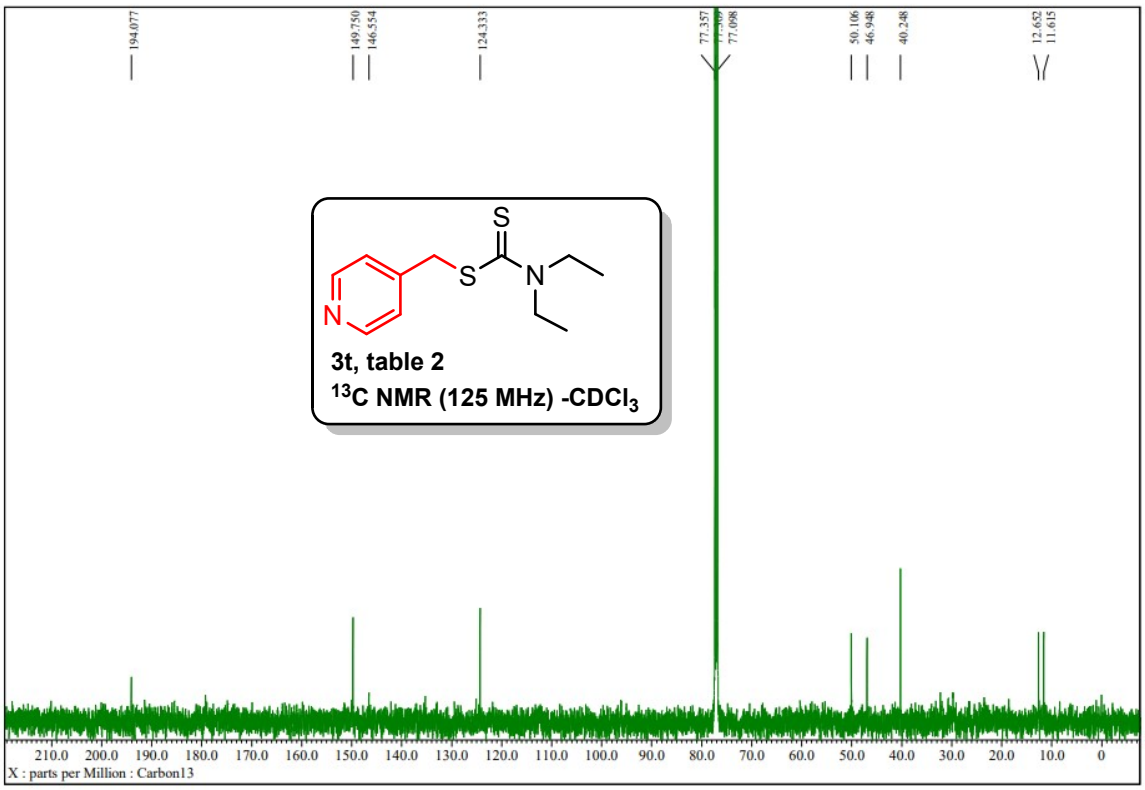
3t, table 2
13C NMR (125 MHz) -CDCl3
X : parts per Million : Carbon13

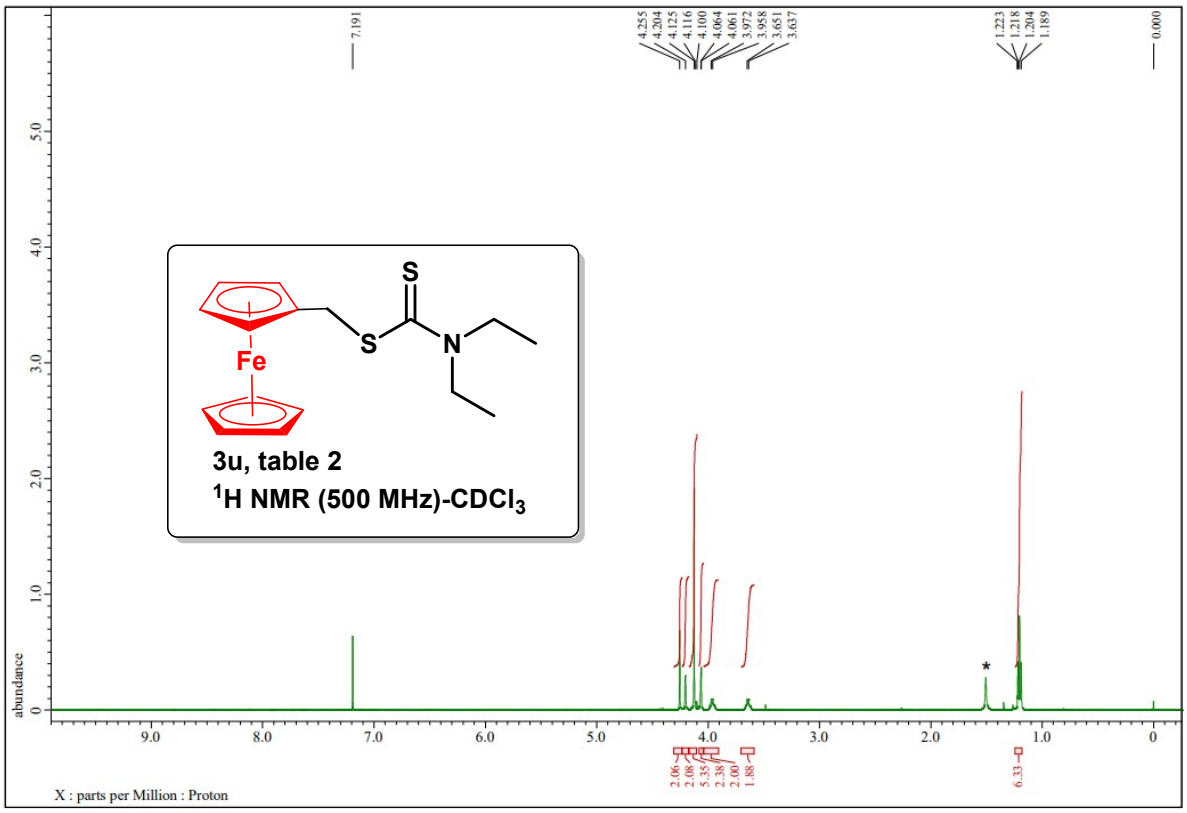

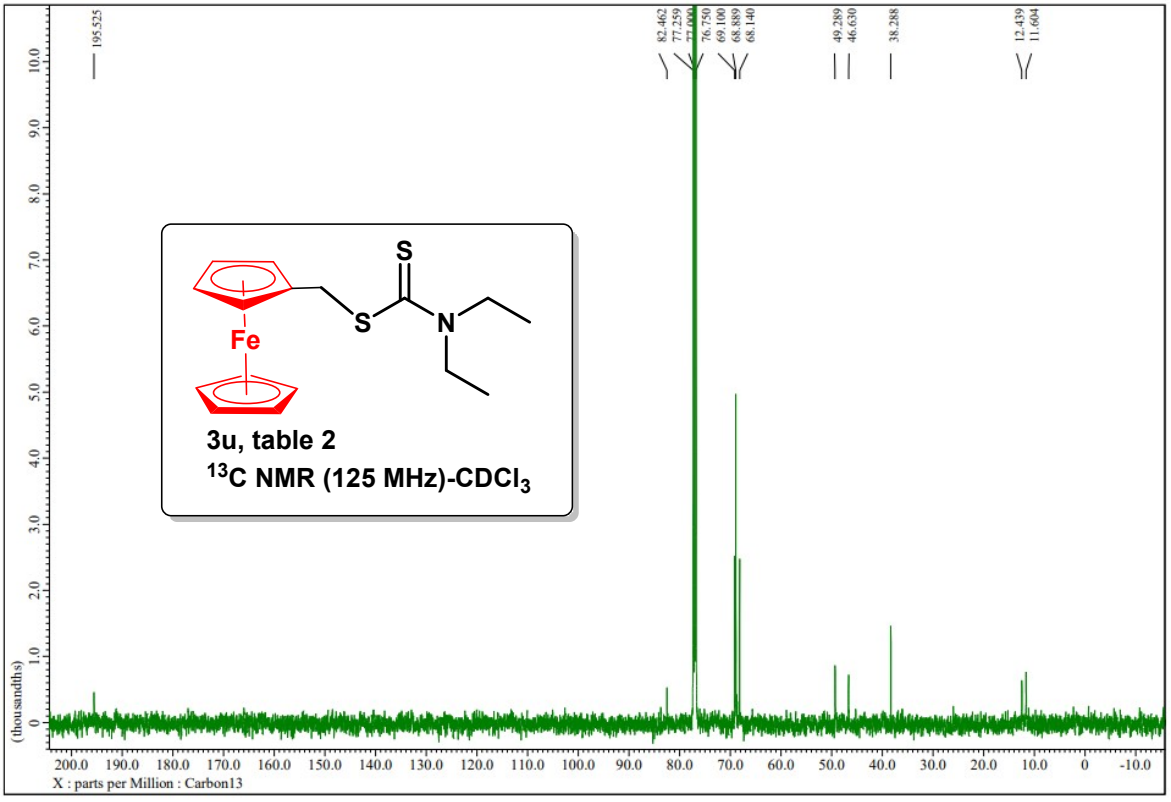

(* moisture, # hexane)

Reference

1. Kumar, N.; Venkatesh, R.; Kandasamy, J. Synthesis of functionalized S-benzyl dithiocarbamates from diazo-compounds via multi-component reactions with carbon disulfide and secondary amines. *Org. Biomol. Chem.* **2022**, *20,* 6766-6770.
2. Krasovskiy, A.; Gavryushin, A.; Knochel, P. Highly stereoselective access to sulfur derivatives starting from zinc organometallics. *Synlett* **2006**, *5,* 0792-0794.
3. Dutta, S.; Saha, A. Iodine mediated direct coupling of benzylic alcohols with dithiocarbamate anions: An easy access of S-benzyl dithiocarbamate esters under neat reaction condition. *Tetrahedron Lett.* **2020**, *61,* 152382
4. Chaturvedi, D.; Ray, S. An efficient, one-pot, synthesis of dithiocarbamates from the corresponding alcohols using Mitsunobu's reagent. *Tetrahedron Lett.* **2006**, *47*, 1307-1309.
5. Wu, Z.; Lai, M.; Zhang, S.; Zhong, X.; Song, H.; Zhao, M. An Efficient Synthesis of Benzyl Dithiocarbamates by Base-Promoted Cross-Coupling Reactions of Benzyl Chlorides with Tetraalkylthiuram Disulfides at Room Temperature. *Eur. J. Chem.* **2018,** *48*, 7033-7036.
6. Azizi, N.; Khajeh, M.; Hasani, M.; Dezfooli, S. An efficient four-component synthesis of dithiocarbamate derivatives. *Tetrahedron Lett.* **2013,** *54*, 5407-5410.
7. Corma, A.; Navas, J.; Rodenas, T.; Sabater, M. J. One-Pot Palladium-Catalyzed Borrowing Hydrogen Synthesis of Thioethers. *Chem. Eur. J.* **2013,** *19*, 17464-17471.
8. (8) Sorribes, I.; Corma, A. Nanolayered cobalt–molybdenum sulphides (Co–Mo–S) catalyse borrowing hydrogen C–S bond formation reactions of thiols or H_2S with alcohols. *Chem. Sci.* **2019**, *10*, 3130-3142.

9. Tirumaleswararao, G.; Vanjari, R.; Singh, K, N. Direct conversion of methylarenes into dithiocarbamates, thioamides and benzyl esters. *Tetrahedron*, **2014**, *70,* 3887-3892.
10. Ahammed, S.; Saha, A.; Ranu B, C. Ruthenium catalyzed one-pot synthesis of S-allyl and cinnamyl dithiocarbamates using allyl and cinnamyl acetates in water. *RSC Adv.* **2012**, 15, 6329-35.
11. Sha, Q.; Wei, Y.Y. One-pot synthesis of S-alkyl dithiocarbamates via the reaction of N-tosylhydrazones, carbon disulfide and amines. *Org. Biomol. Chem,* **2013**, *11*, 5615-5620.
12. Cheng, Y.; Peng, H.Y.; Dong, Z.B. Synthesis of alkyl dithiocarbamates by using thiuram disulfide reagents: A metal-free C (sp3)-S bond formation. *Tetrahedron Lett.,* **2019,** *60*, 617-620.
13. Chen, H.; Zhang, Q.; Zheng, W.; Yang, H.; Zeng, Q. Copper-Catalyzed C− S Coupling of Quaternary Ammonium Salts and Dialkylcarbamodithioic Acid Salts, *Asian J. Org.* Chem. **2020,** *9*, 773-777.
14. (a) Mori, K.; Yamaguchi, K.; Hara, T.; Mizugaki, T.; Ebitani, K.; Kaneda, K. Controlled synthesis of hydroxyapatite-supported palladium complexes as highly efficient heterogeneous catalysts. *J. Am. Chem. Soc.* **2002**, *124,* 11572-11573.
(b) Mondal, S.; Dey, A.; Pal, U. Low temperature wet-chemical synthesis of spherical hydroxyapatite nanoparticles and their in-situ cytotoxicity study. *Adv. Nano Res*. **2016,** *4*, 295.
15. (a) Amedlous, A.; Amadine, O.; Essamlali, Y.; Maati, H.; Semlal, N.; Zahouily, M. Copper loaded hydroxyapatite nanoparticles as eco-friendly fenton-like catalyst to effectively remove organic dyes. *J. Environ. Chem. Eng*. **2021,** *9*, 105501-105515. (b) Thommes, M.; Kaneko, K.; Neimark, A.V.; Olivier, J.P.; Rodriguez-Reinoso, F.; Rouquerol, J.; Sing, K.S.; Physisorption of gases, with special reference to the

evaluation of surface area and pore size distribution*, Pure Appl. Chem.* **2015,** *87*, 1051-1069.

16. Shanmugam, S.; Gopal, B. Copper substituted hydroxyapatite and fluorapatite: Synthesis, characterization and antimicrobial properties, *Ceram. Int.* **2014,** *40*, 15655-15662.
17. (a)Shah, A.T.; Ahmad, S.; Kashif, M.; Khan, M.F.; Shahzad, K.; Tabassum, S.; Mujahid, A. In situ synthesis of copper nanoparticles on SBA-16 silica spheres. *Arab. J. Chem.* **2016**, *9,* 537-541. (b) Liu, P.; Wang, H.; Li, X.; Rui, M.; Zeng, H. Localized surface plasmon resonance of Cu nanoparticles by laser ablation in liquid media. *RSC Adv*. **2015**, *5,* 79738-79745.
18. Guo, J.; Duchesne, P.N.; Wang, L.; Song, R.; Xia, M.; Ulmer, U.; Sun, W.; Dong, Y.; Loh, J.Y.; Kherani, N.P.; Du, J. High-performance, scalable, and low-cost copper hydroxyapatite for photothermal CO_2 reduction. *ACS Catal.* **2020**, *10*, 13668-13681.
19. Amedlous, A.; Amadine, O.; Essamlali, Y.; Daanoun, K.; Aadil, M.; Zahouily, M. Aqueous-phase catalytic hydroxylation of phenol with H_2O_2 by using a copper incorporated apatite nanocatalyst. *RSC Adv*. **2019***, 9,* 14132-14142.
20. Wakamori, S.; Yoshida, Y.; Ishii, Y. Syntheses and Herbicidal Activities of Dithiocarbamates: Part I. Benzyl Esters of N-Substituted Dithiocarbamic Acids and Related Compounds. *Agr. Bioi. Chem*. **1969**, *33,* 1367-1376.
21. Rennar, G.A.; Gallinger, T.L.; Mäder, P.; Lange-Grünweller, K.; Haeberlein, S.; Grünweller, A.; Grevelding, C.G.; Schlitzer, M.; Disulfiram and dithiocarbamate analogues demonstrate promising antischistosomal effects. *Eur. J. Med. Chem*. **2022.** *242*,114641.